Physical connectivity between Pulley Ridge and Dry Tortugas coral reefs under the influence of the Loop Current/Florida Current system

V.H. Kourafalou[1], Y.S. Androulidakis[1], H. Kang[1],

R.H. Smith[2], A. Valle-Levinson[3]

[1]University of Miami/RSMAS, Department of Ocean Sciences, Miami, FL

[2]NOAA-AOML, Physical Oceanography Division, Miami, FL

[3]University of Florida, Civil and Coastal Engineering Department, Gainesville, FL

Submitted to *Progress in Oceanography*

October 2017

Physical connectivity between Pulley Ridge and Dry Tortugas coral reefs under the influence of the Loop Current/Florida Current system

V. Kourafalou, Y. Androulidakis, H. Kang, R. H. Smith, A. Valle-Levinson

Abstract

The Pulley Ridge and Dry Tortugas coral reefs are among the most pristine, but also fragile, marine ecosystems of the continental United States. Understanding connectivity processes between them and with surrounding shelf and deep areas is fundamental for their management. This study focuses on the physical processes related to the connectivity of these reefs. Unprecedented *in situ* time series were used at these specific reef locations, together with satellite observations and numerical simulations, to investigate the dynamics controlling local circulation on the Southwestern Florida Shelf (SWFS) under oceanic influence. The approach of the Loop Current and Florida Current (LC/FC) system to the SWFS slope can induce 0.5 to 1 m/s offshore flows impacting the Pulley Ridge and Dry Tortugas reefs. On the other hand, when the LC/FC system retreats from the slope, onshore flows can carry open-sea waters over the coral reefs. Local formation of cyclonic eddies is possible near the Dry Tortugas reefs in the LC approach case and passage of upstream LC Frontal Eddies is possible in the LC retreat case. Offshore currents ~1 m/s over the SWFS slope were also found during periods of anticyclonic LC Eddy separation. A novel finding is the shedding and northward propagation of mesoscale anticyclonic eddies from the core of the LC along the West Florida Shelf. Eddy shedding may have a broader effect on the dynamics of the shelf around the study reef areas. Long periods of LC/FC domination over these coral reefs (reaching several weeks to months) are characterized

by strong (~1 m/s) along-shelf currents and continuous upwelling processes, which may weaken the slope stratification and bring colder, deeper waters over the shelf-break and toward the shallower shelf region.

Key words: Gulf of Mexico; coral reefs; Pulley Ridge; Dry Tortugas; Florida Keys; numerical modeling; observations; physical oceanography; connectivity

1. Introduction

The Pulley Ridge and Dry Tortugas coral reefs are located near the southwestern edge of the West Florida Shelf in the Gulf of Mexico (GoM; Figure 1a). They are uniquely positioned over the shelf slope where interactions with a powerful boundary current, namely the Loop Current (LC) branch of the Gulf Stream, take place. The LC continues through the Straits of Florida as the Florida Current (FC) branch, along the Florida Keys reef tract, the largest coral reef system in the U.S. Continental margin. The Florida Keys National Marine Sanctuary (FKNMS) encompasses shallow reefs along the Florida Keys and deeper reefs in the Tortugas, under the jurisdiction of the Tortugas Ecological Reserve. About 70 km west of this area lies the even deeper Pulley Ridge reef system, which has the unique characteristics of a mesophotic deep reef environment. Pulley Ridge is the deepest known photosynthetic coral reef in the world and a Habitat Area of Particular Concern, i.e. a high priority area for conservation and management. The Dry Tortugas reefs are shallower than Pulley Ridge, with the Northern Dry Tortugas and Southern Dry Tortugas reefs being atop and at the slope of the Southwest Florida Shelf (SWFS), respectively (Figure 1b).

Although Northern Dry Tortugas and Southern Dry Tortugas are considered part of the same reef system in the Dry Tortugas, they are potentially subject to different dynamics. Furthermore, the circulation pathways connecting them with Pulley Ridge, the Florida Keys reefs and the broader open-sea region are currently unknown. The objectives of this study are to explore: a) similarities and differences on the forcing mechanisms influencing each of the SWFS coral reef regions and b) the physical connectivity pathways between these areas and the downstream shallow reefs of the FKNMS. Results are expected to have implications beyond the understanding of physical

mechanisms. In particular, these circulation processes can be further integrated to biophysical connectivity studies (Sponaugle et al., 2012; Vaz et al., 2016), which are crucial for improving the understanding of coral reef fish replenishment and the management of their fragile ecosystem. The Pulley Ridge mesophotic coral reef ecosystem could export coral larvae to the shallower neighboring reefs, thus acting as a refuge for vulnerable species, assuming recruits survive in the conditions of this new shallow water environment. (Bongaerts et al., 2010).

The study has an observational and a modeling component (Table 1). The observational part includes a unique data set of currents and temperature time series, simultaneously for Pulley Ridge and Dry Tortugas. These were produced from physical oceanography moorings deployed at (Figure 1) Pulley Ridge (PR mooring), as well as over Northern Dry Tortugas (NDT mooring) and Southern Dry Tortugas (SDT mooring) providing hourly water column profiles of current velocity and near-bottom temperature at each site. The modeling part involves numerical simulations, which cover both the local dynamics (around the moorings and the coral reefs of the study area) and the regional dynamics (including the entire GoM and the Straits of Florida). We use our high resolution "Straits of Florida, South Florida and the Florida Keys" Hybrid Coordinate Ocean Model (HYCOM), abbreviated as FKEYS-HYCOM (Kourafalou and Kang, 2012) covering the SWFS and the Straits of Florida (Figure 1a), embedded in the coarser GoM-HYCOM model (Prasad and Hogan, 2007), covering the entire Gulf region. Relevant mesoscale features in the GoM that are expected to impact the study area are as follows.

The major GoM regional circulation pattern is the LC/FC system (part of the Gulf Stream western boundary current), which transports warm oligotrophic water from the Caribbean and

tropical Atlantic Ocean into the GoM. These waters enter through the Yucatan Channel (LC) and exit through the Straits of Florida (FC), continuing to the North Atlantic Ocean as the main branch of the Gulf Stream. In the GoM, the position of the LC varies over time. As the LC extends northward, it eventually starts to form a narrow "neck" and sheds an anticyclonic eddy (LC Eddy, or LCE), which then travels westward. This separation will subsequently result in a dramatic change in the LC, from an "extended" (approaching the northern GoM shelf) to a "retracted" (approaching Cuba and the SWFS) position. These eddy shedding events occur at intervals ranging from 3 to 21 months (Sturges and Leben, 2000), and are associated with the evolution of cyclonic eddies (LC Frontal Eddies or LCFEs) traveling around the LC core (e.g. Hurlburt and Thompson, 1980; Vukovich and Maul, 1985; Vukovich, 1988; Oey et al., 2005; Schmitz, 2005; Chérubin et al., 2006) and contributing to narrowing the LC "neck" (Le Hénaff et al., 2012; Androulidakis et al., 2014). The LCFEs often continue along the FC front, moving into the Straits of Florida and contributing to FC modulations, in synergy with locally produced cyclones adjacent to the Dry Tortugas area (Kourafalou and Kang, 2012). The LC/FC evolution reveals strong inter-annual variability affecting the local shelf circulation over the West Florida Shelf (Fratantoni et al., 1998; He and Weisberg, 2003). The present study is based on the hypothesis that the LC/FC system provides a mechanism for physical connectivity between the Pulley Ridge and Dry Tortugas reef systems and the shallow downstream reefs of the FKNMS. The LC/FC effect on these coral reef regions is also strongly related to the respective temperature changes induced by these warm oceanic waters, which may impact coral survival and growth.

Following the introductory section 1, the methodology is given in section 2, including the description of observations and model simulations. Section 3 presents a model evaluation based on comparisons with measured surface and near-bottom temperature, and moored currents. This section will also discuss the local and regional dynamics: the local circulation features over the SWFS, the regional circulation (LC/FC system), the impact of local eddies on shelf and slope currents, and the wind influence on shelf circulation. Several regional variability events, impacting the connectivity between Pulley Ridge and Dry Tortugas reefs and the LC/FC effects on the shelf-slope vertical structure, are discussed in section 4. Finally, a summary of concluding remarks is presented in section 5.

2. Data and methods

2.1 Observations

2.1.1 Moorings

As part of this study, bottom-mounted Acoustic Doppler Current Profilers (ADCPs) and near-bottom temperature recorders were moored at PR and NDT in August 2012 and at SDT in March 2013 (Figure 1). Instruments at each of the three moorings were maintained annually until their removal in June 2015. This resulted in continuous hourly time series of 27 months for SDT and 34 months for PR and NDT. This unique dataset (first time to have simultaneous current measurements at these reef sites) allowed a synthesis of circulation variability during a relatively extended period. The mooring bottom depths at PR (83.67^{o}W, 24.70^{o}N), NDT (83.09^{o}W, 24.77^{o}N), and SDT (83.15^{o}W, 24.47^{o}N) sites were 69.5 m, 54.5 m, and 66.7 m, respectively. Both PR and SDT moorings are located over the SWFS slope, while the shallower NDT is

located onshore over the shelf (Figure 1b). These observations are used to evaluate the model simulations generated as part of this study with respect to the currents and near-bottom temperature variability for the observational period (2012-2015; see sections 3.1 and 3.2). They are also useful in investigating the local circulation at each deep reef study site (see section 3.2).

The current velocity profilers deployed at each site were Teledyne RD Instruments Workhorse ADCPs, configured to sample hourly and subdivide the water column velocity data into vertical bins of 4 m in depth. A 600 khz unit was installed on the NDT mooring, while the PR and SDT moorings required 300 kHz units, due to the deeper bottom depths at those sites. Current velocity time series from each site were quality controlled and low-pass filtered (at 40 hours, 40 HLP). "Near-surface" velocity data used in the model evaluation represent the currents at a depth range of 9-13 m (PR: ~11 m), 6-10 m (SDT: ~8 m), and 7-11 m (NDT: ~9 m) below the sea surface. These ranges are a function of instrument frequency, bin-size, and site depth, and represent the shallowest data available for each site. "Near-bottom" velocity data used in the analysis are the deepest data available and represent current velocities from 5-9 m (PR: ~63 m and SDT: ~60 m) and 4-8 m (NDT: ~49 m) above the sea floor. Near-bottom temperature time series were recorded from 0.5 m above the sea floor at all sites. A buoy from the National Data Buoy Center is also used to describe the thermal conditions of the upper Keys (PKYF1: 24.918^{o}N, 80.747^{o}W; Figure 1) and to evaluate the model simulations in an area away from our three main moorings in the SWFS region.

2.1.2 Satellite observations

Two satellite datasets were incorporated into the model evaluation. The first dataset is from the Group for High Resolution Sea Surface Temperature (GHRSST; https://www.ghrsst.org/), which includes gridded Sea Surface Temperature (SST) fields. The GHRSST Level 4 SST fields, used in the study, were produced by GHRSST daily Level 2 data (Donlon et al., 2009) covering the model domains (Figure 1a) with horizontal resolution of 1-2 km. These satellite SST fields are used to investigate the inter-annual and seasonal variability of the near-surface temperature over the coral reef study areas and to evaluate the model performance with respect to the model computed near-surface temperature.

The second source of satellite data is from the Archiving, Validation and Interpretation of Satellite Oceanographic Data (AVISO; http://www.aviso.altimetry.fr) produced with support from Centre National d'Etudes Spatiales (CNES; https://cnes.fr). These data include the Sea Level Anomaly (SLA) estimated with altimeters in orbit. We also use the AVISO data updated in 2014 (DUACS 2014), which use the Mean Dynamic Topography (MDT) CNES-CLS13 product. The MDT is added to the SLA to produce Maps of Absolute Dynamic Topography (MADT), which are comparable to the model Sea Surface Height (SSH). MDT represents the time invariant part of the ocean topography, estimated by satellite and *in situ* observations. The MDT is an essential component for capturing dynamical features whose time average has persistent signature, like the LC and FC patterns. The MADT products have a resolution of 1/4° and are generated daily.

2.1.3 Drifters

Surface drifting buoys were deployed at each mooring site during the project research cruises to the study area (2012 to 2015). Satellite-tracked drifters have their drogues centered at 15 m depth to reduce downwind slippage and measure mixed layer currents. Processed trajectory data had 6-hour intervals (Niiler et al., 1995; Lumpkin et al., 2013). The drifters used in this study were released at NDT and SDT sites on 24 August 2013 and 22 August 2013, respectively. Both drifting buoys propagated over the SWFS area, Straits of Florida and Eastern Florida Shelf until 19 October 2013 and 23 September 2013 for NDT (hereafter NDT drifter) and SDT (hereafter SDT drifter) drifters, respectively. The drifter trajectories are used to investigate the FC meandering and respective cyclonic eddies formation and evolution over the coral reef regions (see section 3.4). Comparisons between the drifter speed data and the simulated surface currents are also used to evaluate the ability of the model to simulate regional circulation patterns (e.g. FC evolution). The cross-shore transport, which carries open-sea waters toward the shelf or removes shelf waters away from the reefs is also examined with the use of the surface drifting buoys, released at the mooring sites.

2.2 Hydrodynamic modeling

2.2.1 Description of FKEYS-HYCOM

The local circulation and hydrography of the Pulley Ridge and Dry Tortugas coral reefs are simulated by FKEYS-HYCOM, an implementation of the community HYCOM code (http://hycom.org) with the highest resolution available (1/100^{o} or ~900 m) around the Straits of Florida, South Florida and the Florida Keys

(http://coastalmodeling.rsmas.miami.edu/Models/View/Florida_Keys). HYCOM (Bleck 2002; Chassignet et al., 2003; Halliwell, 2004) is a primitive equation ocean general circulation model supported by code development and operational global/regional simulations in the context of the Global Ocean Data Assimilation Experiment (GODAE) (Chassignet et al., 2007; Kourafalou et al., 2015). FKEYS-HYCOM simulations have been used in the past to investigate the FC meandering and evolution of eddies along the Straits of Florida (Kourafalou and Kang, 2012; Kourafalou et al., 2017), to capture the spatial-temporal scales of circulation influencing larval dispersion in the region between Pulley Ridge and FKNMS (Vaz et al., 2016) and to provide high resolution 7-day forecasts of sea-state around South Florida and the Straits of Florida (http://coastalmodeling.rsmas.miami.edu/).

FKEYS-HYCOM is a free-running model, i.e. it does not assimilate observed data. Data presented in section 2.1 thus offer an independent evaluation. The model has been initialized and nested with a coarser scale model application of HYCOM for the GoM (GoM-HYCOM) which does assimilate observations and uses a GODAE product for boundary conditions, thus providing realistic boundary forcing (see section 2.2.2). The FKEYS-HYCOM topography is derived from the 2 min DBDB2 global data set (Naval Research Laboratory) with a minimum depth of 2 m and with corrected Keys passages through local data (Kourafalou and Kang, 2012). The model employs 26 hybrid vertical layers. For the needs of the current study, the model domain was extended at the north and west boundaries of the implementation by Kourafalou and Kang (2012), from 79^{o}W-83.36^{o}W (previous) to 78^{o}W-84.5^{o}W (current) and from 22.77^{o}N-26.05^{o}N (previous) to 22.18^{o}N-27.51^{o}N (current), see Figure 1a. This was necessary, in order to include the local and regional dynamics over the Pulley Ridge and Dry Tortugas coral reefs. An

additional upgrade is that a high resolution (1/100^o) regional GoM bathymetry developed at Florida State University has been utilized for the extended model domain with a minimum depth of 1 m. Topographic irregularities in Pulley Ridge and around the Dry Tortugas, which were previously missing, are now well represented (Figure 1b). The simulation over the extended domain runs from 2012 to present. Two different three-hourly atmospheric forcing products from the U.S. Navy were used; (1) the Coupled Ocean/Atmospheric Mesoscale Prediction System (COAMPS, Hodur, 1997; Hodur et al., 2002) through 2013 (when it stopped being available) and (2) the NAVy Global Environmental Model (NAVGEM, Metzger et al., 2013), starting in 2014. The former has a spatial resolution of 27 km while the latter has a spatial resolution of 0.5^o until 2015 and 0.281^o starting in 2016. The required atmospheric fields to run the FKEYS-HYCOM are: air temperature at 2 m, shortwave and long wave radiations, specific humidity at 2 m, precipitation, wind speed and wind stress.

2.2.2 Description of GoM-HYCOM

The Gulf of Mexico Hybrid Coordinate Ocean Model (GoM-HYCOM) is used to investigate the regional GoM circulation and provide boundary and initial conditions to the finer FKEYS-HYCOM simulations. It is also based on the HYCOM code and it has been run in near-real time at the Naval Oceanographic Office since 2004, assimilating all available near real time data through the Navy Coupled Ocean Data Assimilation (NCODA; Cummings, 2005). GoM-HYCOM has been used in several GoM studies, either providing boundary and initial conditions to shelf models (Halliwell et al., 2009; Kourafalou et al., 2009; Schiller et al., 2011; Kourafalou and Kang, 2012; Androulidakis and Kourafalou, 2013) or investigating physical or biological processes of the entire GoM region (Prasad and Hogan, 2007; Gierach et al., 2009; Mezić et al.,

2010; Mariano et al., 2011; Le Hénaff et al., 2012; Valentine et al., 2012; Paris et al., 2013). The GoM-HYCOM has a resolution of 1/25^o (~3.6 to 4 km) and extends from 76.40^{o}W to 98^{o}W and from 18.09^{o}W to 31.96^{o}N (Figure 1a) with 20 hybrid layers in the vertical up to 2013 (Prasad and Hogan, 2007; Kourafalou et al., 2009) and with 27 hybrid layers starting in 2014. The minimum and maximum depths are 2 m near the coastline and 7814 m south of Cuba, respectively (Figure 1a). GoM-HYCOM uses cyclic boundary conditions over the Caribbean and Atlantic boundaries extracted from a simulation of the 1/12^o North Atlantic HYCOM, performed during GODAE (see Kourafalou et al., 2009). The atmospheric forcing fields (10 m wind speed, vector wind stress, 2 m air temperature, 2 m specific humidity, surface shortwave and long-wave heat fluxes, and precipitation) are extracted from the three-hourly Navy Operational Global Atmospheric Prediction System (http://www.nrlmry.navy.mil/metoc/nogaps/) reanalysis product (see Prasad and Hogan, 2007) until 2013 and the NAVGEM product from 2014.

3. Results

A data based evaluation of the FKEYS-HYCOM model has been presented by Kourafalou and Kang (2012), including the use of vertical distributions of temperature (monthly ship-borne surveys). They showed that the model sufficiently simulates the vertical structure of the water column (temperature) during all months of the year. They also employed ocean color imagery to show that the model successfully simulated eddy passages along the South Florida reef regions. Additional evaluation using multi-year time series of satellite and *in situ* data has been presented in Kourafalou et al. (2017). They showed that the model captures the variability of both cyclonic and anticyclonic eddies in the Straits of Florida, which they related to the accurate representation of LC/FC undulations. Herein, we further evaluate the model performance, especially over the

coral reefs under study, using a variety of observations, described in section 2. In tandem with the model evaluation, we present the structure of water properties and circulation features that will help elucidate the physical characteristics around the South Florida coral reefs and the connectivity patterns among them.

3.1 Thermal structure around South Florida reefs

Observed and modeled temperature fields are used to study the temperature distribution in the study area and to evaluate model performance. We employ near-bottom temperature measurements collected from the PR, NDT and SDT moorings (2012-2015; Figure 2a) and near-surface temperature measurements from the PKYF1 buoy of the National Data Buoy Center (2009-2016; Figure 2b). We also used GHRSST surface observations, either averaged over the entire FKEYS-HYCOM model domain (2009-2016; Figure 3a) or derived exactly at the locations of the three moorings (2012-2015; Figure 3b). We computed the respective spatial averages from the model and extracted the related simulated time series at the buoy location (near surface temperature) and at each of the mooring sites (SST and temperature at depth, matching the mooring data depths).

The highest mean (averaged over the entire period) near-bottom temperature from both observed (22.58^{o}C) and simulated (22.35^{o}C) values were computed for the shallow NDT mooring (Figure 2a). The lowest Root Mean Square Error (*RMSE*) between the three pairs of time series was also calculated for NDT (~1.28^{o}C). *RMSE* was computed from the daily averaged observations and the respective simulated temperatures at the near-bottom of each mooring and for the entire

observational period. The Pearson correlation coefficient at NDT is high (r_c=0.73), indicating good representation of the temperature variability from summer 2012 to summer 2015 ($r_c \rightarrow 1$: perfect agreement). The p-value is lower than 0.00001 (N=1049), indicating the statistical significance of the correlation (the result is significant at p-value< 0.05; 95% significance). The PR measurements revealed lower mean value (22.39ºC), very close to the simulated one (22.31ºC). The *RMSE* is 0.34ºC higher than the respective NDT comparison, but the correlation coefficient is still positive and relatively high (r_c=0.63). Colder waters were simulated (21.85ºC) and measured (21.52 ºC) at the SDT mooring, where *RMSE* is lower (1.48ºC) than PR. The Pearson correlation coefficient is very close to the NDT correlation (r_c=0.62). Although a point to point comparison between model and mooring data is very challenging, the low errors (*RMSE* values) and high correlation (Pearson coefficients) indicate overall good agreement. The seasonality of the observed near-bottom temperature is well simulated by FKEYS-HYCOM in all three reef locations, where the lower and higher values appeared during spring (~20ºC) and autumn (~24ºC), respectively. Several non-seasonal changes, related mostly to regional oceanic dynamics, are also captured by the model (e.g. a strong drop at the end of summer 2013 and a peak in the beginning of July 2014 at the PR mooring). The surface temperature of the northern Keys (buoy PKYF1) is presented in Figure 2b, where both measured (buoy) and simulated (model) time series reveal a similar variation during the 2009-2016 evaluation period. Significantly low surface temperatures were detected in winter of 2010 from both measured (~16ºC) and simulated (~17ºC) ones, lower than the spatially averaged values (>21ºC) for the entire model domain (Figure 3a). A protracted period of low temperatures was measured and simulated in winter 2013 (<22ºC). A weak but apparently increasing trend is computed for both

time series during the entire 2009-2016 period. The simulated and observed Sen's Slopes, which represent the slope of the trends (Sen, 1968), are almost the same (~0.017).

Figure 3a shows the annual comparison between the simulated and satellite-derived daily SST time series, averaged over the entire model domain. The comparison covers a longer period (2009-2016) to capture the inter-annual variability of the surface temperature over the entire model domain. The Pearson correlation coefficient is significantly high (r_c=0.99), indicating very good agreement of the SST variability for all seasons. Moreover, non-seasonal variation is also well captured by the model. For example, the temperature drops of almost 2^{o}C that occurred in July and August 2012 were well represented by the FKEYS-HYCOM simulation. Similarly, the 1.5^{o}C variations in summer 2010, were also simulated well. The high temperatures of all summers were also accurately computed by the model. Moreover, the model efficiently simulated the low winter temperatures of 2010 and 2015. The lowest winter temperatures occurred in March 2010 and February 2015 (~21^{o}C), while the highest levels for both simulated and measured were in August 2014 (>31^{o}C). The *RMSE* of the entire comparison period is less than half degree (0.48^{o}C), while the *RMSE* values range between 0.63^{o}C and 0.35^{o}C for 2013 and 2014, respectively. The difference between the mean model and GHRSST values is less than the general *RMSE* ($GHRSST_{mean}$ - $Model_{mean}$ = 0.37^{o}C). The comparison between the GHRSST and FKEYS-HYCOM time series at the surface of PR, NDT and SDT mooring sites (Figure 3b) also shows high Pearson correlation coefficients (r_c=0.95) with similar *RMSEs* to the respective errors derived in the bottom of each mooring (Figure 2a). The PR near-surface comparison, which was strongly affected by the LC evolution (see Section 3.3), revealed very small difference between the mean values of the GHRSST and model time series ($GHRSST_{mean}$ -

$Model_{mean}$ = 0.65°C); it also had the lowest *RMSE* between all point-to-point comparisons at the locations of the moorings (~1°C). Short-term variations (non-seasonal changes) of the surface temperature were well captured by the model during both warm (e.g. summer of 2010) and cold (e.g. winter of 2015) seasons. As expected for point-to-point comparisons, the *RMSE* is higher than the respective error from the spatial averaged time series, but the mean values and the high correlation coefficient support the ability of the model to simulate the thermal conditions over the coral reefs under study and the northern Keys. The good agreement between the simulated and satellite-derived SST is remarkable, considering that FKEYS-HYCOM does not assimilate observed data, which could further improve its performance.

The above findings suggest that FKEYS-HYCOM may efficiently reproduce the temperature variability at both near-surface and near-bottom over this topographically complicated region. We note that the efficient simulation of temperature variability is a very important feature of the model at coral reef regions, due to the strong relation between temperature and coral health (Glynn, 1996).

3.2 Local circulation (Southwest Florida Shelf)

The circulation over the West Florida Shelf is determined by a combination of oceanic and atmospheric conditions and their temporal and spatial variabilities (He and Weisberg, 2002). Dynamical processes responsible for the circulation variability include the wind-driven currents, competition between mixing and buoyancy induced by river inputs, and the broader GoM dynamics (Li, 1998). Herein, we examine the local circulation based on *in situ* measurements

and simulated data over the southwestern part of this shelf (SWFS), with a focus on shelf and slope waters surrounding the PR, NDT and SDT mooring sites.

Figures 4 and 5 present the daily variability of near-surface and near-bottom currents, respectively, at the three mooring locations (PR, NDT, and SDT) during the 2013-2014 data period. We focus on these two years because their observational period covers all months (except for the first three months of 2013 at SDT), while only a few months of 2012 and 2015 have current measurements. In addition, 2013-2014 revealed the strongest currents during the entire simulation (FKEYS-HYCOM) and observation period (moorings), especially between March to October 2013 at the PR location (Figures 4 and 6). The model simulated currents were extracted at the same depths of the near-surface and near-bottom ADCP observed currents. Again, we note that such point-to-point current comparisons are extremely challenging. Nevertheless, the overall agreement is very good, both in the magnitude and direction changes in the measured and simulated currents. The LC influence was dominant in 2013, contributing to persistent southward flows (see Section 3.3). We found that both model and observations indicated that southward near-surface currents at PR were 80-90% in 2013 but only 40-60% in 2014, while near-bottom southward currents were about 90% in 2013 and 60% in 2014. We also found that near-bottom measurements had prevailing southward direction at all moorings, with good agreement between model and observations (>65% for 2013 and >55% for 2014). We feel confident to use both data and model time series to discuss the circulation similarities and differences around the three mooring locations.

Between August 2012 (not shown) and March 2013, simulated and observed currents at PR and NDT moorings (no observed currents at SDT in this period) were weak (<10 cm/s) at both near-surface (Figure 4) and near-bottom (Figure 5). In all moorings and years, the upper-ocean currents were generally stronger than the respective deeper ones. Beginning in mid-March 2013 strong off-shelf and along-shelf flows towards the Dry Tortugas were observed at the PR mooring (often >40 cm/s and briefly exceeding 1 m/s; Figure 4). Under such conditions, physical connectivity between Pulley Ridge and the Dry Tortugas may be increased (Vaz et al., 2016). However, the prevailing direction is southwestward for both near-surface (Figure 4) and near-bottom (Figure 5) ADCP currents at NDT, between mid-March 2013 and September 2013. The general southward direction was frequent in both simulated (surface: 42%; bottom: 84.5% of the time) and observed (surface 49%; bottom: 67% of the time) currents, revealing that southward directions prevailed during the entire 2012-2015 period, especially near the bottom at NDT. The PR and SDT moorings reveal high frequency of southeastward currents during the entire study period; both near-surface and near-bottom southeastward currents are strong (>40 cm/s) between March 2013 and October 2013. The strongest simulated currents (>50 cm/s) occurred at the end of June 2013 and early-July 2013 at all locations, as also confirmed by measurements at the respective moorings. A short term but clearly northeastward flow occurred in August 2013 at NDT, indicating the onshore direction of both surface and deeper waters. However, the prevailing currents during the March-October 2013 period we are focusing on were southwestward, carrying the shelf waters offshore. Strong southward currents also occurred at the surface and bottom of PR in summer of 2014 but for a shorter period in comparison to 2013. Generally, 2014 showed significantly weaker currents at all moorings and for both surface and bottom. The strong and persistently southeastward flows at PR indicate the influence of oceanic

currents from the west of the site, as we will discuss in the following sections; there were no tropical storms over the study area during the period of field surveys. Several flow reversals of weaker currents can be seen, that were either related to cold front passages (in winter) or eddy passages (at all seasons).

The Kinetic Energy (KE) per unit mass of the vertically averaged currents shows that the 2013 currents, observed and simulated at the two Dry Tortugas moorings, were typically weaker than the respective currents at PR (Figure 6). The mean KE values, derived from simulated and measured current fields were 1.17 and 1.13 m^2s^{-2} for PR, 0.59 and 0.75 m^2s^{-2} for SDT, and 0.28 and 0.41 m^2s^{-2} for NDT, which showed the weakest simulated and observed currents between the three moorings. The Pearson correlation coefficient, derived between the mean monthly simulated and measured time series of KE, was positive for all moorings, showing its highest values for the shallow NDT mooring (r_c=0.81). The p-value for all correlations was computed for significance level 95% ($p_{95\%}$), which indicates how unlikely a given correlation coefficient will occur given no relationship in the population. In all cases, the $p_{95\%}$ is smaller than the conventional 5% ($p_{95\%}$<0.05), indicating that the correlation coefficient between the time series is statistically significant. SDT reveals the highest p-value, which, however, is also lower than 5% ($p_{95\%}$=0.0487). High coefficient of determination between simulated and measured KE was computed for PR (R^2=0.57) and NDT (R^2=0.66); R^2 approaching unity indicates perfect agreement. The agreement between the two time series was further enhanced in June and July of 2013, when the strongest currents appeared at the PR location. At low KE values, agreement is good at PR and NDT, with deviations from the diagonal (x=y identity line) at SDT, which indicates less agreement. The SDT mooring, located over the southern steep shelf-slope (Figure

1b), is strongly affected by FC meandering and associated frontal cyclonic eddies. Kourafalou and Kang (2012) have shown close synergy between the FC meandering and eddy evolution. They discussed the passage of upstream LCFEs that enter into the Straits of Florida and influence the FC modulations. They also presented a mechanism of local cyclogenesis near the Dry Tortugas, with cyclonic eddies forming when the FC was close to the SWFS slope, effectively blocking the passage of upstream eddies. Kourafalou et al. (2017) expanded these results, showing that the FC meandering is further influenced by anticyclones to the south of FC, propagating eastward along the northern Cuban coast. These processes create a very complex circulation, especially in the vicinity of the SDT mooring site, which makes the point-to-point comparison between the observations and simulations even more challenging. The time series agreement at SDT is still remarkably good, but relatively weaker than for the two other moorings (Figures 4 and 5), revealing lower correlation coefficient (r_c=0.40) and coefficient of determination (R^2=0.07). However, most of the monthly values ranged close to the $x = y$ identity line, showing close average values (Average X~0.75 m^2s^{-2}, Average Y~0.59 m^2s^2; Figure 6).

3.3 Regional circulation (Gulf of Mexico)

The major regional circulation feature that may affect the local circulation over the SWFS is the LC/FC system. We investigate the variability of the LC/FC system and its influence on the circulation around the Pulley Ridge and Dry Tortugas coral reefs during the 2012-2015 study period.

The evolution of the eastward extension of the LC along the S1 Section (Figure 1a), based on the 17 cm SSH contour (Leben, 2005) derived from the realistically forced GoM-HYCOM simulation and the AVISO MADT fields, is presented in Figure 7a. The agreement is very good (which is expected, as this model assimilates available altimeter observations), allowing us to use the regional model results to discuss the locally observed patterns. The simulated LC evolution agrees with the satellite observations, showing strong eastward extension between March 2013 and November 2013 (<84.25^{o}W). Both satellite and simulated polynomial fits of 5th order reveal similar variation during the entire study period. When the LC axis was at an eastward position (near the SWFS slope), the LC southeastward current flowed over the Pulley Ridge coral reef, as measured and also simulated at the PR mooring (Figure 4). The strongest flows are at the end of June 2013 and in the beginning of July 2013, when the easternmost LC extension is observed and simulated (~83.6^{o}W; Figure 7a). The measured and simulated evolution of the mean current KE shows the highest values at the end of June 2013 (>3000 cm^2/s^2; Figure 7b). This is in agreement with findings by He and Weisberg (2003), who showed that the intrusion of the LC over the West Florida Shelf induces a strong southward current along the shelf-break. This current may transport nutrient-rich waters of river origin from the Northern GoM (mainly from the Mississippi) and produce anomalous hydrographic features near the shelf break. On the contrary, the LC was located over the central region away from the shelf (west of 85^{o}W), in summer of 2012, spring of 2014, fall of 2014, and winter of 2015. The lowest KE of the barotropic currents generally appeared during periods of western extension of the LC front, showing a similar variation with the LC extension along the S1 Section. Both simulated (current from FKEYS-HYCOM vs LC longitude from GoM-HYCOM) and observed (current from PR mooring vs LC longitude from AVISO) time series reveal similar positive correlation

coefficients ($r_{KE\text{-}LC\ simulations}$=0.34 and $r_{KE\text{-}LC\ observations}$=0.41), supporting the influence of the LC proximity on the local circulation over the Pulley Ridge coral reef.

The FC is an extension of the LC, flowing in the Straits of Florida between South Florida, Cuba, and the Bahamas, and carrying upper-ocean waters toward the Atlantic Ocean. Although the FC is part of a large-scale current system (Gulf Stream), local changes of the front position within the Straits of Florida are inter-connected with the evolution of remote and locally formed cyclonic, cold-core frontal eddies (Kourafalou and Kang, 2012). The variability in the strength and direction of the FC is discussed based on both FKEYS-HYCOM simulations and drifter trajectories in Section 3.4. In this section, we first focus on the variability of the FC frontal position as the FC enters the Straits of Florida, in order to determine the physical connectivity between the regional FC variability and the local shelf circulation over the Pulley Ridge and Dry Tortugas reefs. Following Kourafalou and Kang (2012), the zonal position of the 20^{o}C isotherm at the depth of 150 m along the 83.5^{0}W meridian is used to determine the FC frontal position (Figure 8). The northernmost position of the FC front along 83.5^{o}W that crosses between the moorings is observed between March 2013 and November 2013 (Figure 8b). This is in agreement with the easternmost position of the LC (Figure 7a), indicating the domination of the LC/FC system dynamics over the South Florida coral reef region. The northward FC extension reached 24.4^{o}N in mid-March 2013, in agreement with the eastward LC shift over the shelf (approaching 84^{o}W; Figure 7a). The northernmost latitude reached by the FC front was estimated in June 2013 (~24.6^{o}N), when the FC was over the shelf slope (Figure 8b) and the strongest (Figure 7b) southeastward (Figure 4) currents occurred at PR. The LC migrated far eastward at the end of June (~83.75^{o}W; Figure 7a), more than at any other time during the entire study

period. However, a short-term (~5 days) southward excursion of the FC was revealed during the first days of July 2013, in agreement with a respective reduction of the observed and simulated current magnitude at the PR mooring and the westward migration of the LC along the S1 Section (~84.25^{o}W; Figure 7a). Generally, 2013 exhibited an annual mean FC frontal position that reached the furthest North (FC_{mean}=24.22^{o}N), as compared to the rest of the study period, in agreement with the long-lasting LC eastern location. The southernmost mean FC frontal position along 83.5^{o}W was estimated in 2014 (FC_{mean}=23.85^{o}N). The southernmost position of the 20^{o}C isotherm at 150 m was computed during April-May 2014 (<23.5^{o}N), indicating that the FC front was well separated from the SWFS. Further southward separation of the FC front also occurred in September 2014, March 2015 and August 2015, while northward FC frontal displacements were simulated in January, July, October, and December of 2014 (Figure 8c). Month-long periods of northern FC location are also evident in 2015 (e.g. April, June-July and September-November; Figure 8d).

The main onshore and offshore flow across the shelf-break (toward and away from the Pulley Ridge and Southern Dry Tortugas coral reefs) takes place across the isobath of 100 m between the two respective moorings (S2 Section; Figure 1b). The daily-integrated transport across the S2 Section and over the entire depth of 100 m (Q_{S2}) for all study years is presented in Figure 8 (black line). The 2012 Q_{S2} is small without strong negative (offshore) or positive (onshore) peaks (<0.2 Sv), due to limited FC variation during the entire 2012. The mean FC frontal position for 2012 is 23.9^{o}N, while the 4-year period (2012-2015) mean is 23.97^{o}N. Relatively large volume transports, and generally offshore transport with a few onshore peaks are computed during 2013; large negative transport is observed in June (-0.02 Sv), July (-0.025 Sv) and late-August (-0.03

Sv), indicating the offshore removal of shelf waters toward the Straits of Florida, in tandem with the most northern FC position. The northward FC displacement (north of 24.4^{o}N) over the edge of the coral reef areas contributes to the offshore removal of shelf waters. On the other hand, the sharp southward withdrawal of the FC front in the beginning of July 2013 (24.1^{o}N) is associated with a respective onshore flow across the shelf-break and toward the coral reefs (0.05 Sv), which lasted only a few days, in agreement with the short-term FC withdrawal. There is an inverse correlation (r<0) between the two time series (latitude of FC frontal position and Q_{S2} transport) for almost all years, showing higher negative coefficient for 2013 (r_{2013}=-0.30) and 2014 (r_{2014}=-0.31), and lower for 2012 (r_{2012}=-0.10) and even positive correlation for 2015 (r_{2015}=0.04). The $p_{95\%}$ for the correlation coefficient for 2013, which is the most important year with respect to the LC/FC system interaction to the local circulation, is less than 0.0001 (<0.05), indicating the statistical significance of the comparison. Generally, the annual mean position of the FC front in 2013 is the highest (FC_{mean}=24.22^{o}N) of the 4-year period, staying persistently far north and almost over the shelf slope. This supported the long periods of offshore flow across the shelf-break, in agreement with the near-surface and near-bottom measurements at PR and SDT moorings, which showed prevailing southward flows during 2013 (Figures 4 and 5).

Offshore transport also prevailed in 2014, reaching a maximum of -0.03 Sv in July 2014, following the respective northward FC displacement (from 23.5^{o}N at the end of June to 24.4^{o}N in mid-July). The correlation between the FC frontal location and the transport in 2014 is the highest of the entire 4-year period (r_{2014}=-0.31). Similar variation of across-slope flows is observed in 2015 (Figure 8d), with relatively low offshore transport until August (<0.02 Sv). Increased offshore and onshore transports are observed in early October and December 2015,

respectively. Both negative and positive transport levels are related to the northward (from 23.5^{o}N in mid-August to 24.4^{o}N in September) and southward (from 24^{o}N at the end of November to 23.5^{o}N in December) FC displacement, respectively. The location of the FC front is linked to the shelf waters flowing over the Pulley Ridge and Dry Tortugas coral reefs. In particular, the northward FC shift is associated with offshore transports larger than -0.01 Sv.

It is noted that further distance of FC and LC from the shelf region is associated with less offshore flows, but not necessarily with more onshore flows across the shelf-break. The southward FC shift (23.3^{o}N; Figure 8c) and the extended westward shift of LC (85.6^{o}N; Figure 7a) in late August and early September 2014 were associated with weak offshore transports (-0.006 Sv), but not with a respective onshore transport (Figure 8c). On the other hand, a few significant onshore flows are also detected during northern extensions of the FC front along the 83.5^{o}N meridian (e.g. 0.015 Sv in mid-August 2014 and 0.01 Sv in June 2015). The impact of local eddies related to the FC meandering is probably responsible for this variability (see section 3.4). Several atmospheric and other oceanic conditions, such as prevailing winds over the shelf and eddy evolution along the Straits of Florida, may be responsible for potential discrepancies from the prevailing relationship between the frontal location and cross-shore transport. These conditions may play an additional role on the local circulation of the coral reefs study region and the transport across the shelf-break.

3.4 Impact of local eddies on shelf and slope currents

Kourafalou and Kang (2012) suggested that northward FC frontal position, combined with southwestward shelf currents, create current shear that favors the local formation of cyclonic eddies over the Dry Tortugas area, which then move downstream to fill the cyclonic FC curvature. Moreover, they showed that southward FC displacements near the western entrance of the Straits of Florida were associated with remote cyclones entering from the GoM.

Herein, we examine two groups of cases that differ in terms of the FC proximity to the mooring area, the presence of eddies along the FC immediately downstream or upstream and the prevailing wind conditions. We have chosen examples with local (Group 1) or remote (Group 2) cyclones present near the reef areas (Figure 9). Winds vary, although easterly components prevail in most cases. The first two cases (Group 1; Figures 9a and 9b) have ~-0.02 Sv offshore flow across the shelf-break and northern FC frontal position in June 2013 (Figure 8b) and July 2014 (Figure 8c). In both cases, the FC northern extension is around 24.4^{o}N, affecting the local circulation over the coral reefs areas under study. The two cases of Group 2 show a weak (~0.01 Sv) but apparent onshore transport (Figure 8c). An onshore transport is detected in late-March 2014 (0.012 Sv) when the FC front was located significantly further south (~150 km, 23.25^{o}N) from the shelf-break (Group 2; Figure 9c). However, the other case of Group 2 with northern displacement of the FC (~24^{o}N) (no curvature or meandering of the FC in the Straits), but with negligible offshore flow (almost zero transport), is observed in mid-August 2014 (Figure 9d).

The major difference between Group 1 and Group 2 is related to the LC/FC pattern, which influences the FC evolution and the formation of the cyclonic meandering of the FC over the Dry Tortugas region. In Group 1, the LC is displaced toward the East (Figure 7a), allowing the

formation of a downstream frontal FC cyclone between the Dry Tortugas islands and Western Florida Keys, south of the 100 m isobath. Although southeasterly winds prevailed and caused a respective northward near-surface flow over the SWFS on 6 June 2013, the front between the southeastward FC flow and a cyclonic eddy, located between the Dry Tortugas moorings and the Western Florida Keys (Figure 9a), carried shelf waters offshore across the shelf-break between the PR and SDT sites (Figure 8b). Similarly, the meandering of the FC enhanced the formation of a downstream cyclonic eddy on 19 July 2014 (Figure 9b) and a respective offshore transport across S2 (Figure 8c). On the other hand, in the absence of downstream FC cyclones between the Florida Keys and Dry Tortugas, and despite the northern FC location, offshore transport across S2 was limited and a weak onshore flow (~0.012 Sv; Figure 8c) took place (18 August 2014; Figure 9d). The evolution of a cyclonic eddy over the Pulley Ridge region affected the local circulation across the shelf-break and advected waters toward the shelf (Figure 8c), despite the easterly winds prevailing over the area (Figure 9d). Southward displacements of the FC front near the western entrance of the Straits of Florida were observed in March and April 2014 (Figure 8c). The FC front started to move southward in February, reaching its southernmost position in March; it approached Cuba, around 23.2^{o}N on 1 April 2014, and remained over this southern region during the first half of the month. Meanwhile, the transport across the shelf-break became positive (~0.01 Sv), indicating onshore transport that is apparently related to the loss of FC influence near the shelf-break. A clear cyclonic eddy is apparent on 30 March 2014 at the southwest of the coral reefs region and the north of the FC (Figure 9c). This southward moving cyclone, which originated from the GoM along the LC, followed the southward FC displacement, in agreement with Kourafalou and Kang (2012). The eddy's downstream propagation continued and it reached the western entrance of the Straits of Florida by late-March

2014. The cyclonic circulation over this area carried surface waters toward the shelf and affected the transport across the shelf-break near the Pulley Ridge and Dry Tortugas coral reefs. During these two cases (Group 2), the cyclone downstream propagation reduced the offshore transport and even caused onshore transport, despite the differences in the FC frontal location (southward on 30 March 2014 and northward on 18 August 2014). These results suggest that eddy propagation is a factor influencing across-shelf flow between the PR and SDT moorings, in addition to LC/FC system modulations.

The trajectories of the two drifters, deployed at the end of August 2013 near the NDT and SDT moorings (section 2.2.3), are characterized by the circulation described in Group 1. This circulation happens when LC and FC are close to the coral reefs and cyclonic eddies can be formed locally, with the northern FC front around the Pulley Ridge location, between the Dry Tortugas and FKNMS areas (Kourafalou and Kang, 2012). The FC curvature near the Dry Tortugas and the westward coastal currents enhanced the local generation of a cyclonic eddy prior to the drifters deployment. The eddy induced offshore transport was -0.03 Sv (Figure 8b). This eddy moved southwestward between the PR and SDT mooring sites on 1 September 2013 (Figure 10a). The speed of the NDT drifter was less than 0.25 m/s on 1 September; both drifters showed low speeds over the shelf in agreement with the simulated surface currents over the shelf. However, they were entrained by the southeastward FC along the shelf-break and were carried away from the mooring sites together, exhibiting higher speeds (0.5 m/s), following the southeastward moving cyclonic eddy on 6 September (Figure 10b). The strong eastward currents along the FC are also confirmed by the simulations. The cyclone became enlarged over the area surrounding (24^{o}N, 82.5^{o}W) and entrained both drifters, spinning them cyclonically twice, with

speed ranging between 0.25 and 0.5 m/s (e.g. 6 September and 13 September). The NDT drifter followed an extended cyclonic circulation and was trapped in a second cyclone that was formed off the Dry Tortugas on 1 October (Figure 10d). The northwestward propagation of the drifter (~0.25 m/s) agrees with the simulated northwestward surface currents that prevailed over the shelf. The SDT drifter was swept away by the FC toward the Atlantic Ocean. The second cyclonic eddy increased the offshore flow across the S2 Section (~-0.015 Sv; Figure 8b). The transport became onshore (~0.04 Sv) during the cyclone's southeastward displacement on 10 October 2013 (Figure 10e); the NDT drifter moved to the South and then propagated to the East, following the cyclonic eddy and the FC flow, increasing its speed (0.5-0.75 m/s), in agreement with the simulated general circulation over the area. Finally, the NDT drifter exited the Straits of Florida on 17 October, following the general Gulf Stream evolution (not shown). It is noted that FKEYS-HYCOM efficiently simulated the regional and local circulation over the moorings region, in agreement with the drifter trajectories and speed presented in Figure 10. Both drifter speeds and model currents show a decrease in the FC magnitude along the Straits between September (~1 m/s) and mid-October (~0.5 m/s). The two drifters followed the flow from the shelf toward the open sea, were entrained in the FC meandering and followed the local cyclones north of the FC and along the SWFS, as presented in model results. The drifter trajectories and the simulated currents confirmed the contribution of the FC meandering and the associated eddy formation on the offshore removal of shelf waters from the Pulley Ridge and Dry Tortugas coral reefs toward the Straits of Florida.

3.5 Wind effects on shelf circulation

As presented in Figure 9 along with the general shelf near-surface circulation (upper model layer) over the SWFS, winds were prevailing from the Southeast (e.g. 6 June 2013; Figure 9a), the North (e.g. 19 July 2014; Figure 9b) and the West (e.g. 30 March 2014; Figure 9c). The current fields of all cases showed a respective surface circulation determined by Ekman dynamics. Southeasterly winds advected the shelf waters toward the North over the entire study region and northwesterly winds produced a generally southward flow, carrying waters toward the study areas of coral reefs and Florida Keys. The southwesterly winds over the SWFS induced a respective eastward surface flow toward the Western Florida coast (Figure 9c). In all cases, the inner-shelf surface circulation was strongly determined by the prevailing wind conditions.

Figure 11 presents the differences for the winds and the vertically averaged currents between the Northern Dry Tortugas reef (located over the shallower shelf region) and the Pulley Ridge reef (located over the shelf-break). The winds at both NDT and PR mooring locations during the entire study period (2012-2015), derived from the COAMPS/NAVGEM fields (section 2.2), revealed highest occurrence in the southwestward direction (PR: 44.6% and NDT: 52.7%), with prevailing magnitudes between 5 to 10 m/s. Magnitudes >10 m/s occurred mainly for the southwestward direction in both mooring sites. The prevailing current direction at the NDT mooring site was southwestward for both measured (46%) and simulated (56.8%). The prevailing direction of the PR mean currents was found to be southward with higher occurrence frequency for southwestward (observation: 33.2% and model: 23.9%) than for southeastward (observation: 27.3% and model: 53.4%), especially for strong magnitudes. Currents >40 cm/s were found at PR, especially under the LC effect, while the majority of the strongest currents have a 30-40 cm/s range at the shallower NDT mooring site due to the wind prevailing

conditions (Figure 11). Low occurrence frequency was detected in the northwestward and northeastward directions. These estimates are in agreement with the near-surface and near-bottom current evolution shown in Figures 4 and 5. All moorings showed high southward occurrence frequency at both near-surface and near-bottom, as presented in section 3.2. These results confirm the impact of regional circulation (LC and FC) over the outer-shelf coral reef of Pulley Ridge, while the shallower Northern Dry Tortugas area is mostly affected by the wind-induced circulation over the SWFS.

4. Discussion

Following the presentation of results on the local and regional circulation impacting the observed and simulated variability around and over the SWFS coral reefs, we further discuss the processes influencing reef connectivity. Specific events are employed to investigate the variability of the regional circulation that impacts the coral reefs under study. We also discuss the impact of the LC/FC system on stratification characteristics of the slope waters and the upwelling processes around the reefs.

4.1 Regional variability events impacting connectivity between Pulley Ridge and Dry Tortugas

The modulations of the LC/FC front have a significant impact on the local circulation of the Pulley Ridge and Dry Tortugas regions, as presented in section 3.3. The FC perturbations also affect the formation and evolution of eddies (Tortugas eddies) over the SWFS and the Straits of Florida (Fratantoni et al., 1998). The FC exhibits a meandering pattern within the Straits of

Florida, in synergy with cyclonic frontal eddy evolution (Kourafalou and Kang, 2012). The variability of the simulated and measured vertically averaged current velocity at the PR mooring for 2013 and 2014 is presented in Figure 12. We focus on these two years due to the continuous availability of measurements at the PR mooring site. Thirteen characteristic events have been selected, representing the connectivity of the LC system and the circulation indicated by currents measured at PR during the 2013-2014 period (Table 2). These events were chosen based on the current magnitudes at PR in relation to the variability of the regional circulation patterns, such as the LC system. Seven events related to weak currents and six events related to strong currents are discussed. There is a positive correlation between the LC eastward extension and the KE of the PR barotropic current during the entire study period, as presented in Figure 7. We now investigate the magnitude of the PR vertically averaged current in relation with the regional LC system evolution inside the GoM and its specific characteristics. We characterize the LC system evolution by the extension of the northern boundary of the LC core (maximum latitude reached) and the LC eddy field, which includes: the detachment (*d*), attachment (*a*) and re-attachment (*ra*) of the anticyclonic LCE (also called a "ring"), the cyclonic LCFEs (*c*) and the release of northward (along the West Florida Shelf slope) anticyclonic eddies from the LC core (*A*).

The LCE separation process is not a single abrupt event, but a gradual pulling away, with parts of the flow connecting the LC core to the separating ring for a significant part of its travel time to the West (Sturges et al., 1993). Table 2 presents 6 characteristic events, when the LCE detached from the main LC body and its core retreated below 25.5^{o}N (E2, E4, E5, E8, E11 and E13). The separation events are identified by the significant changes in the northward LC extension (Leben, 2005; Le Hénaff et al., 2012). In all of these 6 events, the PR current was significantly strong,

exhibiting velocities that exceeded 40 cm/s and in some cases reached the level of 80 cm/s (Table 2). Two events with strong currents occurred in spring of 2013 (E2 and E4) when the LCE detached from the main body and the LC was restricted over the western side of the Straits of Florida in a very low latitude (24~25^{o}N). The strongest PR currents (>70 cm/s) were measured and simulated at the end of June 2013 (E5; Figure 12). During this period the northern boundary of the LC core was located near 24.5^{o}N, the LCE was temporarily detached from the main LC body toward the Gulf interior and a smaller anticyclonic eddy was also detached from the LC body and traveled northward along the West Florida Shelf slope (Figure 13). This is an important finding, relating the LC proximity to the SWFS slope to increased current flows over the Pulley Ridge reef. The LC position was influenced by the LCE detachment. The shedding of the relatively smaller, northward anticyclones along the West Florida Shelf is a less studied process, which will be further discussed below. The southward LC restriction (~25^{o}N), following respective LCE detachments, also coincided with strong PR currents in early September 2013 (E8), July 2014 (E11) and late September 2014 (E13). Again, the main feature that characterized these strong current events over the Pulley Ridge reef is the LCE detachment from the LC main body.

Another new finding is that the re-attachment of the LCE (which usually enhances the northward extension of the LC) is related to a reduction in the PR current velocities. The weakest currents occurred in February 2013 (<10 cm/s), when the LC attached to the LCE reached its northernmost position (29^{o}N; E1). LCEs may detach and re-attach several times between eddy shedding events (Sturges and Leben, 2000), which show a period of approximately 10.5 months (Jacobs and Leben, 1990), although this may vary inter-annually (Leben, 2005; Le Hénaff et al.,

2012). In 2013, this is the case in May (E3; Table 2) and in early-July (E6; Table 2), when the detached LCE re-attached on the LC main body and enhanced its extension towards the North (>27^{o}N). The weak currents were sustained for 15 days until mid-July (Figure 12a), when the LC extended more to the North. Both simulated and measured KE showed a substantial reduction during July, following a significant peak at the end of June (Figure 7b). Similarly, the re-attachment of the LCE increased the northward extension of the LC over 28^{o}N in August 2014 (E12; Figure 13), when very weak currents were measured over the Pulley Ridge coral reef (Figure 12b).

Finally, a less studied regional process was observed during the study period and was found to influence the PR currents. Mesoscale anticyclonic eddies (marked with "A") were shed from the main LC core and traveled north along the West Florida Shelf slope. These are generally smaller in size than the LCE, starting at ~50 km diameter and reaching 100km and occasionally up to 150 km. These eddies have been briefly mentioned by Zavala-Hidalgo et al. (2006) during their modeling study on LCE shedding variability. We found that this process can occasionally result in sustained shedding of anticyclones from the LC core. This was the case during summer to early fall in 2013. A current weakening (~20 cm/s) occurred in August 2013, when the LC system evolved along the West Florida Shelf (E7; Table 2, Figure 13) and led to the release of anticyclonic eddies (A1, A2) from the LC, reaching the northern GoM on a northward pathway over the shelf slope. Very low velocities were also measured and simulated in September 2013 (E9; Table 2) when the LC extended along the West Florida shelf and finally released successive anticyclonic eddies ("A") over the eastern GoM. The PR vertically averaged currents weakened in mid-November (Figure 12a), showing the lowest simulated levels on 22 November 2013 (<5

cm/s; E10). The LC released anticyclonic eddies ("A") continuously during this period, forming a domain of increased eddy activity along the slope of the West Florida Shelf reaching the latitude of 28^{o}N (Table 2). The position of the LC and the anticyclonic eddies may contribute on the variability of the barotropic circulation over the southwestern coral reefs, showing mainly weak currents but also high short-time peaks of velocity, following a respective retreat of the LC main body over the SWFS region.

The extension of the LC along the Western Florida shelf may result to the attenuation of the PR currents similar to the re-attachment of the LCE on main LC body over the central Gulf. However, the detachment of anticyclonic eddies from the LC (LCE or "A" eddies) may lead to a significant retreat of the LC (to the south of the 25^{o}N latitude) and a simultaneous increase of the PR currents. The late May 2013 detachment of LCE (E4), which was influenced by the LCFE C1 intrusion from the North, was followed by a successive shedding of several "A" anticyclones along the West Florida Shelf slope in mid-June (10 June 2013; Figure 13); currents at PR temporarily weakened (<40 cm/s; Figure 12a). A northern GoM LCFE (C2) was formed in the proximity of the Mississippi Delta and remained over the region during June 2013 blocking the LCE from moving more to the North. The C1 cyclone remained northeast of the LCE, while C3 (which originated from the Campeche Bank continental shelf) propagated northeastward and contributed to the separation of an anticyclone (A1) from the LC. The next event was a southward LC retreat near the SWFS (25 June 2013; Figure 13). The highest velocities at the PR mooring site were measured during this period (E5; Figure 12a). The sequence of the events during June includes an initial strengthening of the currents in early June (LCE detachment), the weakening of the currents in mid-June (extension of LC along the shelf under the LCFEs effect)

and the strengthening of the PR currents at the end of June (release of "A" eddies). In early July 2010, Smith et al. (2014) measured a strong southward flow between Pulley Ridge and Dry Tortugas areas, while the northern edge of the LC was impinging upon the southwest Florida shelf at ~24.75°N and 84.0°W, near the mesophotic Pulley Ridge reef in a similar fashion (their Figure 4).

The Campeche Bank LCFEs (as C3) also play an important role on the separation processes of LCE (Zavala-Hidalgo et al., 2003; Schmitz, 2005; Le Hénaff et al., 2012; Athié et al., 2012; Androulidakis et al., 2014). Their intensification and northward propagation towards the LC may be enhanced by upwelling events over the Campeche shelf during summer months (Androulidakis et al., 2014). In addition to C3, another LCFE formed over the Campeche Bank in mid-July 2013 (C4; Figure 13) and also propagated toward the North, along the periphery of the young LC. It reached 24ºN by mid-August 2013. In addition to C1, another northern GoM LCFE (C2) moved southward and reached the western boundary of the anticyclonic activity area along the West Florida Shelf slope by mid-August 2013. These two LCFEs, one from the North and one from the South, kept the main LCE away from the LC and restrained the LC northward extension along the shelf. The northward LC extension reached the northwestern GoM and formed "A" anticyclonic eddies along 86ºW (E7; Figure 13). The extended spreading of LC along the West Florida Shelf narrowed the "neck" of the LC, reducing its energy over the southwestern coral reefs and the velocity of PR currents in mid-August 2013 (~20 cm/s; Figure 12a).

Two cases with similar LC conditions (extended LC), but with different local circulation at the SWFS region were detected in the summer of 2014. The strongest PR currents of 2014 were measured and simulated in mid-July (E11; Figure 12b). The detachment of the LCE led to the southern retraction of the LC body, which thus concentrated over an area covering the coral reefs under study (12 July 2014; Figure 13). The C5 and C6 LCFEs originated from the northeastern GoM and the Campeche Bank, respectively, and contributed to narrowing the LC "neck", which was previously extended over the central Gulf in June 2014; very weak currents occurred during June over the Pulley Ridge area (Figure 12b). The narrowing of the LC "neck" led to the widening of its body to the west of the SWFS (5 July 2014; Figure 13), increasing the PR currents in the beginning of July (Figure 12b). The final detachment was followed by the strongest PR currents in mid-July 2014 (>50 cm/s). C6 remained over the northwestern boundary of the LC, keeping the LCE detached from the main body (20 July 2014; Figure 13). However, the attenuation of C6 and the significant northward extension of the LC at the end of July and in early-August led to the re-attachment of the LCE over the northern GoM. A fully-extended LC over the central GoM with a very narrow "neck" is observed away from the Pulley Ridge region in mid-August (15 August; Figure 13), keeping the current magnitudes in very low levels (E12; Figure 12b). It is noted that the local circulation over the coral reef study region is related to the LC system attributes, especially to the LCE shedding events, which are strongly determined by the LCFEs traveling around the periphery of the LC.

The formation and evolution of the "A" anticyclonic eddies along the slope of the West Florida Shelf were found strongly correlated with the LC structure over the coral reefs region, affecting the PR currents variability. A long period of extensive LC spreading along the shelf slope is

observed in November and December 2013 (Figure 14), corresponding to event E10 (Table 2 and Figure 12a). A large and intensive LCFE (C; Figure 14) was detected in both AVISO and GoM-HYCOM over the central Gulf, which restricted the LC induced anticyclonic circulation at the eastern GoM, over the West Florida Shelf slope. A detached anticyclonic LCE has propagated away from the LC body and remained over the western GoM during the entire event period. The eastward shift of the LC was accompanied by a series of anticyclones (A3 on 22 November and A4 on 6 December; Figure 14) that were shed from the LC core and propagated northward along the shelf slope, forming an elongated anticyclonic warm patch. The C cyclonic eddy remained over the central region, keeping the LC system over the West Florida Shelf region. The anticyclonic eddy formation (*A* eddies) is also confirmed by SST satellite observations (GHRSST; Figure 14). High temperatures are also simulated by GoM-HYCOM along the shelf (>30^{o}C), indicating the origin of the northward traveling anticyclonic eddies, in agreement with the GHRSST fields (we remind that GoM-HYCOM assimilates SST satellite observations). During the formation of "A" eddies in November-December 2013, the PR currents were generally weak (Figure 12a), but they showed a few high peaks due to the position of the LC and the continuous releases of these anticyclonic eddies from the LC main body. Strong northward currents were simulated by GoM-HYCOM over the LC extension along the West Florida Shelf slope on 22 November 2013 (Figure 15a). The clear anticyclonic circulation of the A3 eddy is also observed at the tip of the LC, while weaker currents are detected over the coral reef region. The formation of a second anticyclonic eddy (A4; Figures 14 and 15b) induced a change on the LC extension and intensified the currents over the coral reef region in the beginning of December. Extensive anticyclonic activity prevailed along the West Florida Shelf slope; besides the distinctive A3 and A4 eddies, anticyclonic cores are observed all along the 100

m isobath on 6 December 2013 (Figure 15b). These patterns are characterized by high SST and are located north of the main LC body (Figure 14). The LC main body propagated eastward, advecting warmer waters along the shelf slope.

The extension of the LC along the West Florida Shelf slope, detected on 22 November 2013, influenced the bottom of the shelf slope, affecting directly the coral reefs of the region. This is important, as the bottom temperature conditions, which are strongly related to the LC patterns, are determinative for the reef resilience. The temperature difference between 22 November (extended LC along the shelf slope) and 1 November (retracted LC) is greater than 3^{o}C along the western shelf, due to the LC intrusion over the area (Figure 15c). The release of the anticyclonic eddies along the shelf, followed by the withdrawing and intensification of the LC on 6 December, increased the bottom temperature only over a smaller area over the SWFS (dT_{bottom}>4^{o}C; Figure 15d). However, the difference is negative along the shelf-break between the Dry Tortugas and Pulley Ridge areas, due to upwelling processes (see Section 4.2). Moreover, negative difference (~-2^{o}C) was also computed along the northern slope (~26^{o}N), indicating that the warm A4 anticyclone did not affect the bottom temperature conditions after its release from the LC main body, due to its relatively shallow eddy depth.

4.2 LC/FC impact on slope stratification

We showed that the LC/FC system plays an important role on the dynamics of the SWFS and determines the local circulation over the Pulley Ridge and Dry Tortugas coral reefs, especially over the shelf slope. The shelf-break currents (PR and SDT) are strongly influenced by the

offshore currents, whereas the mid-shelf currents (NDT) are largely controlled by the prevailing local winds. Weisberg et al. (2000) showed that the inner-shelf of the West Florida Shelf responds in a classical Ekman-geostrophic manner and the variability of stratification and alongshore geometry may affect the inner-shelf responses to wind forcing. The LC intrusions onto this shelf actually have both barotropic and baroclinic components (He and Weisberg, 2003). An important effect is LC-induced upwelling, a slope process that has also been shown in other areas under boundary current influence. Smith (1983) showed that upwelling may occur over the Eastern Florida Shelf when the northward Gulf Stream boundary current comes in contact with the continental shelf; temperature minima follow increases in current speed even over further offshore shelf areas rather than in response to the coastal upwelling-favorable wind field. This is to be distinguished from wind-induced coastal upwelling as in Hsuesh and O'Brien (1971).

The monthly evolution of the Brunt-Väisälä frequency (*N* stratification frequency; sec^{-1}) at the PR mooring site, as derived from the FKEYS-HYCOM simulations and averaged over the entire water column, is presented in Figure 16a. The stratification frequency was computed to investigate the vertical mixing ability of the water masses located between the surface and the bottom.

$$N^2 = \frac{(-g / \rho_o)(\rho_1 - \rho_2)}{\Delta z}$$

where g is the gravitational acceleration (9.806 ms^{-2}), ρ_o is the initial ambient sigma-theta (1022.4 kgm^{-3}), ρ_1 and ρ_2 are the upper and lower layer mean density respectively, and Δz is the thickness of each model layer in order to calculate the mean stratification frequency of the water

column. As expected, high values (strong stratification) occurred during summer and low values (weak stratification) occurred during winter and spring (black line in Figure 16a). However, the removal of the seasonal cycle (red line in Figure 16a) revealed significant differences with profound alterations from May 2013 to November 2013, when the LC front reached its easternmost location and influenced the local circulation. The lower *N* levels of the seasonally adjusted time series (<0.004 sec^{-1}) were computed in August 2013, when the LC was over the coral reef study areas (strong LC influence). The respective *N* levels with the seasonal cycle were significantly higher (~0.008 sec^{-1}). The weakening of the stratification is strongly related to the oceanic boundary current (LC/FC system) that induced upwelling along the slope and determined the local circulation of the study region. On the contrary, the removal of seasonality did not reveal any significant modification of the stratification during the summer of 2014, when the LC/FC system was away from the SWFS; both seasonal and seasonally adjusted values revealed respective high peaks.

Two characteristic events (E8 in late-August and early-September 2013 and E12 in August 2014; Table 2 and Figure 12) were identified during these two periods. Strong eastward velocities of the FC were simulated very close to the shelf-break and the coral reefs on 28 August 2013 (>150 cm/sec; Figure 16b); the temperature distribution along the S3 Section (Figure 1a) shows that upwelling occurred during this period, when colder waters moved towards the upper layers over the shelf slope; lower temperatures were also evident over the coral reefs. In addition, very cold waters were measured and simulated at the bottom of all moorings during August 2013 (<20^{o}C, Figure 2a). This strong drop in temperature was probably related to the intrusion of the upwelled waters over the coral reefs. This was not the case in August 2014, when the stratification was

stronger (Figure 16a); higher temperatures were evident over the coral reefs and neither LC/FC influence nor upwelling were observed (Figure 16b).

The Hovmöller diagram of the vertical distribution of temperature at the H1 site, located between the PR and SDT mooring sites over the shelf slope (Figure 1b), presents the two characteristic periods of LC influence discussed in Figure 16 (Figure 17). All summers are characterized by higher temperature in the upper 100 m, while very lower temperature and homogenous water column are observed during all winters. However, the appearance of LC/FC over the slope induced two significant upwelling incidents: one at the end of May 2013 (E4; Figure 17a) during the early phase of the LC influence (the 24^{o}C isotherm moved from 80 m to 45 m) and a more profound one when the 24^{o}C isotherm raised up to 50 m depth, at the end of August 2013 (E8; Figure 17a). The upwelling formation is also confirmed by the strong upward velocities (>0.15 cm/s) that occurred at several depths during this period (Figure 16b). On the contrary, vertical advection was small or even downward from 2012 until the spring of 2013. It was also attenuated beyond 2013, after the strong LC influence over the slope. The absence of the LC/FC formed a period of strong stratification (Figure 16a) with very high temperature values over the upper-ocean and no significant isotherm lifts in summer of 2014, when LC/FC influence was absent (Figure 17a). In contrast to the summer of 2013, when strong upward velocities occurred, especially between 50 m to 100 m, the summer of 2014 did not exhibit any upward, upwelling-related velocities, indicating negligible vertical advection (e.g. E12; Figure 17b).

4.3 Implications on biophysical connectivity

We have shown that oceanographic features, such as eddies and fronts, may form between the shelf waters and the open ocean over the SWFS coral reefs. These have been found to enhance and concentrate productivity, generating high-quality patches that dispersive marine larvae may encounter in the plankton (Shulzitski et al., 2016). The biological processes over the unique community of the SWFS reefs are strongly related to the variability of the physical local dynamics that are influenced by the regional circulation patterns, especially over the deep Pulley Ridge coral reef. The location of this reef is unique, because it is commonly bathed by the LC/FC system (onshore transport; Figure 8), while it is also near the continental shelf. Thus, the reef can be under the influence of relatively clear and warm LC waters, but also under the influence of slope upwelling events that can bring cooler, nutrient-rich waters (Hine et al., 2008). The connectivity between the deep coral communities (e.g. Pulley Ridge and Southern Dry Tortugas) and the shallower reef areas (e.g. Northern Dry Tortugas and the Florida Keys) may play an important role in the recovery of shallow reef areas by functioning as refugia from the repeated disturbances that have affected these reefs (Bongaerts et al., 2010). Upwelling events are also enhanced by the LC evolution along the shelf slope, as it was presented for summer 2013 (Section 4.2), when the LC was located close to the reefs and induced significant upwelling, bringing colder waters over the shelf. Based on satellite SST and chlorophyll *a* data, Jarrett et al. (2005) confirmed the influence of the LC on Pulley Ridge. The northward (onshore) flows are also common over the Pulley Ridge region (Figure 8), supporting the transport of the larvae over the mid-shelf (Vaz et al., 2016), where the balance between buoyancy-driven and wind-driven flows drives the transport (Weisberg et al., 2005; Kourafalou et al., 2009; Liu and Weisberg, 2012). The physical dynamics over the SWFS coral reefs also control the temperature water levels, which cause coral reef bleaching; a leading factor responsible for large-scale coral

reef bleaching is elevated sea temperatures (Glynn, 1996). More than 50% live coral is observed in 60–75 m of water due to the LC/FC support that provides warm and clear waters to the deep Pulley Ridge reef, although less than 2% of surface light is available to the reef community (Jarrett et al., 2005). However, the LC related upwelling events can bring colder deeper waters over the reefs, opposing this effect.

The LC/FC system is often in close proximity to Pulley Ridge and downstream reefs around the Dry Tortugas and the Florida Keys, presenting a physical connectivity mechanism through the interaction of coastal/shelf and offshore flows. Both drifter and model results showed that there is strong connectivity between the water masses that originated in the Pulley Ridge region and the downstream reefs, through the FC pattern and its related cyclonic eddies (Figure 10). Vaz et al. (2016) employed the physical model presented herein to perform biophysical simulations of larval dispersal. They found that the Pulley Ridge mesophotic reef larvae are subject to sporadic one-way transport to the shallow-water reefs of the Dry Tortugas and the Florida Keys. They concluded that, while biophysical Pulley Ridge connections may be persistent between locations along the Dry Tortugas and the FKNMS, they tend to be highly variable in time, and fluctuate in accordance to oceanographic conditions prevailing during the spawning events. These findings are in agreement with the strong variability of the local circulation presented in Section 3.2. Direct export of bicolor damselfish larvae can take place from Pulley Ridge to coral reefs of the FKNMS, particularly to the western Florida Keys reefs along the LC/FC corridor (Vaz et al., 2016). Alternatively, larvae spawned at Pulley Ridge can be entrapped by eddies and transported over the shallower bathymetry of the Florida Keys, an indirect connectivity pathway. The synergy of physical and biological processes along the Florida Keys reefs has been discussed by

Sponaugle et al. (2005), where the role of eddies in the recruitment of coral reef fishes was first discussed. In follow-up studies (Sponaugle et al., 2012; Shulzitski et al., 2015; 2016), related details were explored, especially how eddies increase the larvae survival advantage and contribute to the population replenishment. For instance, Shulzitski et al. (2016) have shown that wrasses (e.g. Thalassoma bifasciatum), residing outside of eddies in the oligotrophic FC during warm periods, experienced high mortality and only the slowest growers survived early larval life. The above studies have concentrated on the Florida Keys reefs. The observations and modelling presented herein offer a novel physical background to explore broader biophysical connectivity among South Florida reefs. Furthermore, they can support broader studies on the connections between mesophotic and shallow reef systems.

5. Conclusions

We have elucidated the physical processes influencing circulation around the Pulley Ridge and Dry Tortugas coral reefs. We have focused on a multi-month period when the circulation around the reefs was largely influenced by regional currents and eddy passages impinging on the shelf break. We showed that when the Loop Current and Florida Current (LC/FC) system was near the Southwestern Florida Shelf (SWFS) slope, offshore flows impacted Pulley Ridge and local formation of cyclonic eddies near the Dry Tortugas reefs was possible. When the LC/FC system was away from the slope, passage of upstream Loop Current Frontal Eddies (LCFEs) was facilitated. The mesoscale circulation is largely controlled by the LC/FC system variability, which includes these oceanic currents and the associated eddies. These results have provided *in situ* observational evidence, corroborated by model results, in support of findings by Kourafalou

and Kang (2012) and Kourafalou et al. (2017), which were based on simulations, satellite and drifter data.

Our results quantified and characterized the strong variability among the neighboring SWFS reefs. The area around Northern Dry Tortugas, which is relatively inshore, was the only one found to have circulation influenced by winds. He and Weisberg (2003) showed that although the shelf-break currents of the WFS are largely LC-controlled, the inner-shelf currents are mostly controlled by the local winds. However, their findings focused further North than this study. Hetland et al. (1999, 2001) suggested that LC impacts on the southernmost extent of the WFS during the "young" phase of the LC eddy-shedding cycle generate only a 10 cm/s trans-shelf southward current along the broader WFS. Our study has refined these results and has given an unprecedented focus on the SWFS circulation. Although the LC effects on the central WFS are brief and intermittent (Meyers et al., 2001), we showed that the SWFS circulation around the Pulley Ridge and Dry Tortugas reefs is strongly related to the LC and FC evolution.

The LC Eddy (LCE) separation events, which abruptly limit the northward LC extension, are strongly related to the formation of southward currents over the Pulley Ridge slope. The local circulation over the coral reefs study region is related to almost all LC system attributes and especially to the LCE shedding events, which are strongly determined by the LC Frontal Eddies (LCFEs) traveling around the periphery of the LC. A novel result is that mesoscale anticyclonic eddies may also shed from the main LC core and travel north along the WFS slope. The LC extension along the WFS, strongly related to strong LCFEs over its western boundary, and the release of successive anticyclonic eddies affect the dynamics over the coral reef regions. The

LC/FC system also affects the slope stratification of the SWFS and determines the formation and evolution of upwelling events, which may carry colder waters over the Pulley Ridge and Southern Dry Tortugas coral reefs. A long period of LC/FC domination over the coral reef study areas in 2013 was characterized by strong along-shelf currents and continuous upwelling processes, which weakened the slope stratification and brought colder deeper waters over the shelf-break and toward the shelf. The LC/FC evolution plays a key role on the dynamics of the region, affecting the physical conditions, which have an impact on the environmental conditions and on the health of the coral reef ecosystem. The physical connectivity among South Florida deep and shallow reef systems presented in this study has, therefore, important implications on biophysical connectivity. The observed and modeled persistent periods of south to southeastward currents over the reef areas indicate that the Pulley Ridge deep reef system may act as refugia for the shallower reef environments along the Florida Keys.

Acknowledgments

The study was funded by the National Oceanic and Atmospheric Administration (NOAA) Center for Sponsored Coastal Ocean Research under award NA11NOS4780045 to the University of Miami (Project Title: “Connectivity of the Pulley Ridge - South Florida Coral Reef Ecosystem”). The project represents a collaboration of more than thirty scientists at ten different universities and two Federal laboratories (NOAA’s Atlantic Oceanographic and Meteorological Laboratory, AOML, and Southeast Fisheries Science Center) pooling their expertise through NOAA’s Cooperative Institute for Marine and Atmospheric Studies at the University of Miami, in coordination with the Cooperative Institute for Ocean Exploration, Research, and Technology at Florida Atlantic University. The drifters were provided by the Global Drifter Program at NOAA/AOML. Ryan Smith acknowledges partial support from the Physical Oceanography Division at NOAA/AOML. Additional support to the UM/RSMAS authors on Gulf of Mexico dynamics was made possible through a grant to V. Kourafalou by the Gulf of Mexico Research Initiative (award GOMA 23160700). We thank M. Le Hénaff (University of Miami/CIMAS) for fruitful discussions on the results of this study.

References

Androulidakis, Y.S. and V.H., Kourafalou, 2013. On the processes that influence the transport and fate of Mississippi waters under flooding outflow conditions. *Ocean Dyn.*, 63(2-3), pp.143-164.

Androulidakis, Y.S., V.H., Kourafalou and M., Le Hénaff, 2014. Influence of frontal cyclones evolution on the 2009 (Ekman) and 2010 (Franklin) Loop Current Eddy detachment events. *Ocean Sci.*, 10, 947–965, doi:10.5194/os-10-947-2014.

Athié, G., J. Candela, J., Ochoa and J., Sheinbaum, 2012. Impact of Caribbean cyclones on the detachment of Loop Current anticyclones. *J. Geophys. Res.*, 117, C03018, doi:10.1029/2011JC007090.

Bleck, R., 2002. An oceanic general circulation model framed in hybrid isopycnic-Cartesian coordinates. *Ocean Model.*, 4(1), pp.55-88.

Bongaerts, P., Ridgway, T., Sampayo, E.M. and O., Hoegh-Guldberg. 2010. Assessing the 'deep reef refugia'hypothesis: focus on Caribbean reefs. *Coral reefs*, 29(2), pp.309-327.

Chassignet, E.P., L.T., Smith, G.R., Halliwell and R., Bleck, 2003. North Atlantic simulations with the Hybrid Coordinate Ocean Model (HYCOM): Impact of the vertical coordinate choice, reference pressure, and thermobaricity. *J. Phys. Oceanogr.*, 33(12), pp.2504-2526.

Chassignet, E.P., H.E., Hurlburt, O.M., Smedstad, G.R., Halliwell, P.J., Hogan, A.J., Wallcraft, R., Baraille and R., Bleck, 2007. The HYCOM (hybrid coordinate ocean model) data assimilative system. *J. Mar. Syst.*, 65(1), pp.60-83.

Chérubin, L.M., Y., Morel and E.P., Chassignet, 2006. Loop Current ring shedding: the formation of cyclones and the effect of topography, *J. Phys. Oceanogr*., 36, 569–591.

Cummings, J.A., 2005. Operational multivariate ocean data assimilation. *Q. J. Roy. Meteorol. Soc.*, 131(613), pp.3583-3604.

Donlon, C.J., K.S., Casey, I.S., Robinson, C.L., Gentemann, R.W., Reynolds, I., Barton, O., Arino, J., Stark, N., Rayner, P., Le Borgne and D., Poulter, 2009. The GODAE high resolution sea surface temperature pilot project. *Oceanography*, 22(3), pp.34-45.

Fratantoni, P.S., T.N., Lee, G.P., Podesta and F., Muller‐Karger, 1998. The influence of Loop Current perturbations on the formation and evolution of Tortugas eddies in the southern Straits of Florida. *J. Geophys. Res.: Oceans*, 103(C11), pp.24759-24779.

Glynn, P.W., 1996. Coral reef bleaching: facts, hypotheses and implications. *Global Change Biol.*, 2(6), pp.495-509.

Gierach, M.M., B., Subrahmanyam and P.G., Thoppil, 2009. Physical and biological responses to Hurricane Katrina (2005) in a 1/25 nested Gulf of Mexico HYCOM. *J. Mar. Syst.*, 78(1), pp.168-179.

Halliwell, G.R., 2004. Evaluation of vertical coordinate and vertical mixing algorithms in the HYbrid-Coordinate Ocean Model (HYCOM). *Ocean Model.*, 7(3), pp.285-322.

Halliwell, G.R., A., Barth, R.H., Weisberg, P.J., Hogan, O.M., Smedstad and J., Cummings, 2009. Impact of GODAE products on nested HYCOM simulations of the West Florida Shelf, *Ocean Dyn.*, 59, 139–155, doi:10.1007/s10236-008-0173-2.

He, R., and R.H., Weisberg, 2002. West Florida shelf circulation and temperature budget for the 1999 spring transition. *Cont. Shelf Res.*, 22(5), pp.719-748.

He, R., and R.H., Weisberg, 2003. A Loop Current Intrusion Case Study on the West Florida Shelf. *J. Phys. Oceanogr.*, 33(2), pp.465-477.

Hetland, R., Y., Hsueh and D., Yuan, 2001. On the decay of a baroclinic jet flowing along a continental slope. *J. Geophys. Res.: Oceans*, 106(C9), pp.19797-19807.

Hetland, R.D., Y., Hsueh, R.R., Leben and P.P., Niiler, 1999. A loop current‐induced jet along the edge of the West Florida Shelf. *Geophys. Res. Lett.*, 26(15), pp.2239-2242.

Hine, A.C., R.B., Halley, S.D., Locker, B.D., Jarrett, W.C., Jaap, D.J., Mallinson, K.T., Ciembronowicz, N.B., Ogden, B.T., Donahue and D.F., Naar, 2008. Coral reefs, present and past, on the West Florida shelf and platform margin. *Coral Reefs of the USA*, pp.127-173.

Hodur, R.M., 1997. The Navy Research Laboratory's Coupled Ocean/Atmosphere Mesoscale Prediction System (COAMPS). *Mon. Weather. Rev.*, 125, 1414-1430.

Hodur, R.M., X., Hong, J.D., Doyle, J., Pullen, J., Cummings, P., Martin and M.A., Rennic, 2002. The Coupled Ocean/Atmosphere Mesoscale Prediction System (COAMPS). *Oceanography*, 15(1), 88-98.

Hsuesh, Y. and J.J., O'Brien, 1971. Steady coastal upwelling induced by an along-shore current. *J. Phys. Oceanogr.*, 1(3), 180-186.

Hurlburt, H. and J.D., Thompson, 1980. A numerical study of Loop Current intrusions and eddy shedding, *J. Phys. Oceanogr.*, 10, 1611–1651.

Jacobs, G.A. and R.R., Leben, 1990. Loop current eddy shedding estimated using Geosat altimeter data. *Geophys. Res. Lett.*, 17(13), pp.2385-2388.

Jarrett, B.D., A.C., Hine, R.B., Halley, D.F., Naar, S.D., Locker, A.C., Neumann, D., Twichell, C., Hu, B.T., Donahue, W.C., Jaap and D., Palandro, 2005. Strange bedfellows—a deep-water hermatypic coral reef superimposed on a drowned barrier island; southern Pulley Ridge, SW Florida platform margin. *Mar. Geol.*, 214(4), pp.295-307.

Kourafalou, V.H., G., Peng, H., Kang, P.J., Hogan, O.M., Smedstadt, R.H., Weisberg, M.O., Baringer and C.S., Meinen, 2009. Evaluation of global ocean data assimilation experiment products on nested simulations with the Hybrid Coordinate Ocean Model, *Ocean Dyn.*, 59, 47–66, doi:10.1007/s10236-008-0160-7.

Kourafalou, V. H. and Kang, H., 2012. Florida Current meandering and evolution of cyclonic eddies along the Florida Keys Reef Tract: Are they interconnected? *J. Geophys. Res.: Oceans*, 117(C5).

Kourafalou V.H., P., De Mey, M., Le Hénaff, G., Charria, C.A., Edwards, R., He, M., Herzfeld, A., Pasqual, E., Stanev, J., Tintoré, N., Usui, A., Van Der Westhuysen, J., Wilkin and X., Zhu, 2015. Coastal Ocean Forecasting: system integration and validation. *J. Oper. Oceanogr.*, doi:10.1080/1755876X.2015.1022336.

Kourafalou, V.H., Y.S., Androulidakis, H., Kang and M., Le Hénaff, 2017. The dynamics of Cuba anticyclones (CubANs) and interaction with the Loop Current / Florida Current system. *J. Geophys. Res.: Oceans*, doi:10.1002/2017JC012928.

Leben, R.R., 2005. Altimeter‐Derived Loop Current Metrics. Circulation in the Gulf of Mexico: Observations and Models, edited by: Sturges, W. and Lugo-Fernandez, A., American Geophysical Union, 181-201.

Le Hénaff, M., V.H., Kourafalou, Y., Morel and A., Srinivasan, 2012. Simulating the dynamics and intensification of cyclonic Loop Current Frontal Eddies in the Gulf of Mexico. *J. Geophys. Res.: Oceans*, 117(C2).

Li, Z., 1998. Upwelling circulation on the west Florida continental shelf, Ph.D. thesis, 309 pp., Univ. of South Fla., St. Petersburg.

Liu, Y., and R.H., Weisberg, 2012. Seasonal variability on the west Florida shelf. *Prog. Oceanogr.*, 104, pp.80-98.

Lumpkin, R., S., Grodsky, L., Centurioni, M., Rio, J., Carton and D., Lee, 2013. Removing spurious low-frequency variability in drifter velocities. *J. Atmos. Oceanic Technol.,* 30, pp. 353–360. http://dx.doi.org/10.1175/JTECH-D-12-00139.1.

Mariano, A.J., V.H., Kourafalou, A., Srinivasan, H., Kang, G.R., Halliwell, E.H., Ryan and M., Roffer, 2011. On the modeling of the 2010 Gulf of Mexico oil spill. *Dynam. Atmos. Ocean*, 52(1), pp.322-340.

Metzger, E.J., A.J., Wallcraft, P.G., Posey and O.L., Smedstad, 2013. The Switchover from NOGAPS to NAVGEM 1.1 Atmospheric Forcing in GOFS and ACNFS. NRL/MR/7320--13-9486. Available at http://hycom.org/dataserver/navgem .

Meyers, S.D., E.M., Siegel and R.H., Weisberg, 2001. Observations of currents on the west Florida shelf break. *Geophys. Res. Lett.*, 28(10), pp.2037-2040.

Mezić, I., S. Loire, V.A., Fonoberov and P., Hogan, 2010. A new mixing diagnostic and Gulf oil spill movement. *Science*, 330(6003), pp.486-489.

Niiler, P.P., A., Sybrandy, K. Bi, P., Poulain and D., Bitterman, 1995. Measurements of the water-following capability of holey-sock and TRISTAR drifters. *Deep Sea Res. Part I*, 42, pp. 1951–1964. http://dx.doi.org/10.1016/0967-0637(95)00076-3.

Oey, L.Y., T., Ezer and H.C., Lee, 2005. Loop current, rings and related circulation in the Gulf of Mexico: A review of numerical models and future challenges. Circulation in the Gulf of Mexico: Observations and Models, edited by: Sturges, W. and Lugo-Fernandez, A., American Geophysical Union, 31–56.

Paris, C.B., J., Helgers, E., Van Sebille and A., Srinivasan, 2013. Connectivity Modeling System: A probabilistic modeling tool for the multi-scale tracking of biotic and abiotic variability in the ocean. *Environ. Model. Softw.*, 42, pp.47-54.

Prasad, T.G. and P.J., Hogan, 2007. Upper‐ocean response to Hurricane Ivan in a 1/25 nested Gulf of Mexico HYCOM. *J. Geophys. Res.: Oceans*, 112(C4).

Schiller, R.V., V.H., Kourafalou, P., Hogan and N.D., Walker, 2011. The dynamics of the Mississippi River plume: Impact of topography, wind and offshore forcing on the fate of plume waters. *J. Geophy. Res.: Oceans*, 116(C6).

Schmitz, W.J., 2005. Cyclones and westward propagation in the shedding of anticyclonic rings from the Loop Current. Circulation in the Gulf of Mexico: Observations and Models, Geophys. Monogr. Ser, vol. 161, edited by W. Sturges and A. Lugo-Fernandez, pp. 241–261, American Geophysical Union, Washington, D. C.

Sen, P.K., 1968. Estimates of the regression coefficient based on Kendall's tau. *J. Am. Stat. Assoc.*, 63(324), pp.1379-1389.

Shulzitski, K., S., Sponaugle, M., Hauff, K., Walter, E.K., D'Alessandro and R.K., Cowen, 2015. Close encounters with eddies: oceanographic features increase growth of larval reef fishes during their journey to the reef. *Biol. Lett.*, 11(1), p.20140746.

Shulzitski, K., S., Sponaugle, M., Hauff, K.D., Walter and R.K., Cowen, 2016. Encounter with mesoscale eddies enhances survival to settlement in larval coral reef fishes. *Proc. Natl. Acad. Sci.*, 113(25), pp.6928-6933.

Smith, N.P., 1983. Temporal and spatial characteristics of summer upwelling along Florida's Atlantic shelf. *J. Phys. Oceanogr.*, 13(9), 1709-1715.

Smith, R.H., E.M., Johns, G.J., Goni, J., Trinanes, R., Lumpkin, A.M., Wood, C.R., Kelble, S.R., Cummings, J.T., Lamkin and S., Privoznik, 2014. Oceanographic conditions in the Gulf of Mexico in July 2010, during the Deepwater Horizon oil spill. *Cont. Shelf Res.*, 77:118-131. doi:10.1016/j.csr.2013.12.009.

Sponaugle, S., T.N., Lee, V.H., Kourafalou and D., Pinkard, 2005. Florida Current frontal eddies and the settlement of coral reef fishes. *Limnol. Oceanogr.,* 50: 1033-1048.

Sponaugle, S., C., Paris, K., Walter, V.H., Kourafalou, E., D' Alessandro, 2012. Observed and modeled larval settlement of a reef fish to the Florida Keys. *Mar. Ecol. Prog. Ser.* 453: 201–212, doi: 10.3354/meps09641.

Sturges, W., J.C., Evans, S., Welsh and W., Holland, 1993. Separation of warm-core rings in the Gulf of Mexico. *J. Phys. Oceanogr.*, 23(2), pp.250-268.

Sturges, W. and R., Leben, 2000. Frequency of ring separations from the Loop Current in the Gulf of Mexico: A revised estimate. *J. Phys. Oceanogr.*, 30(7), pp.1814-1819.

Valentine, D.L., I., Mezić, S., Maćešić, N., Črnjarić-Žic, S., Ivić, P.J., Hogan, V.A., Fonoberov. and S., Loire, 2012. Dynamic autoinoculation and the microbial ecology of a deep water hydrocarbon irruption. *Proc. Natl. Acad. Sci.*, 109(50), pp.20286-20291.

Vaz, A.C., C.B., Paris, M.J., Olascoaga, V.H., Kourafalou, and H., Kang, 2016. The perfect storm: match-mismatch of bio-physical events drives larval reef fish connectivity between Pulley Ridge and the Florida Keys. *Cont. Shelf Res.,* 125, 136-146, http://dx.doi.org/10.1016/j.csr.2016.06.012.

Vukovich, F.M., 1988. Loop Current boundary variation, *J. Geophys. Res.: Oceans*, 93, 15,585–15,591, doi:10.1029/JC093iC12p15585.

Vukovich, F.M. and G.A., Maul, 1985. Cyclonic eddies in the eastern Gulf of Mexico, J. Phys. *Oceanogr*., 15, 105–117, doi:10.1175/1520- 0485(1985)015<0105:CEITEG>2.0.CO;2.

Weisberg, R.H., B.D., Black and Z., Li, 2000. An upwelling case study on Florida's west coast, *J. Geophys. Res.: Oceans*, 105(C5), pp.11459-11469.

Weisberg, R.H., R., He, Y., Liu and J.I., Virmani, 2005. West Florida shelf circulation on synoptic, seasonal, and interannual time scales. Circulation in the Gulf of Mexico: Observations and Models, *Geophys. Monogr. Ser*, vol. 161, edited by W. Sturges and A. Lugo-Fernandez, pp.325-347.

Zavala-Hidalgo, J., S.L., Morey and J.J., O'Brien, 2003. Cyclonic eddies northeast of the Campeche Bank from altimetry data, *J. Phys. Oceanogr.*, 33, 623–629.

Zavala-Hidalgo, J., S.L., Morey, J.J., O'Brien and L., Zamudio, 2006. On the Loop Current eddy shedding variability. *Atmósfera*, 19(1), pp.41-48.

Table 1 Data and methods used in the study. Abbreviations: Pulley Ridge (PR); Northern Dry Tortugas (NDT); Southern Dry Tortugas (SDT); Gulf of Mexico (GoM); National Data Buoy Center (NDBC); Sea Level Anomaly (SLA); Sea Surface Temperature (SST); Sea Surface Height (SSH); Group for High Resolution Sea Surface Temperature (GHRSST); Archiving, Validation and Interpretation of Satellite Oceanographic Data (AVISO); Straits of Florida, South Florida and the Florida Keys (FKEYS) and Gulf of Mexico (GoM) Hybrid Coordinate Ocean Model (HYCOM).

Tool		Period	Coverage	Resolution Frequency	Parameters	Data Assimil.
Moorings	PR NDT SDT	2012-2015 2012-2015 2013-2015	Shelf slope Middle Shelf Shelf slope	Hourly Hourly Hourly	Current Temperature	-
NDBC buoy	PKYF1	2009-2016	Upper Keys	Hourly	SST	-
Drifters		2013	Shelf Straits	6-hourly	Trajectory	-
AVISO		2012-2015	GoM	1/4° Daily	SLA	-
GHRSST		2009-2016	GoM	1-2 km Daily	SST	-
FKEYS-HYCOM		2009-2016	Shelf Straits	1/100º 6-hourly	SSH Current Temperature Salinity	No
GoM-HYCOM		2012-2015	GoM	1/25º Daily	SSH SST	Yes

Table 2 Connectivity Events selected according to the relationship between the variability of the Loop Current (LC) system and currents at the Pulley Ridge (PR) mooring location during the 2013-2014 period, as derived from the GoM-HYCOM simulation fields (LC system characteristics) and FKEYS-HYCOM fields (current velocity at PR). The LC system variability is characterized from: 1) the LC core extension (maximum latitude reached); 2) the LC eddy field, which includes: the detachment (d), the re-attachment (ra), and the attachment (a) of the Loop Current Eddy (LCE); and the formation of northward (along the WFS slope) anticyclonic eddies from the LC core (A). Bold letters indicate the events with current velocities higher than 40 cm/s (which are marked by LC core extension below 25.5ºN and detached LCE).

Event #	Period	LC core	LCE	PR current
1	1 Feb – 28 Feb 2013	29ºN	a	<10 cm/s
2	1 Mar – 31 Mar 2013	**24ºN**	**d**	**~50 cm/s**
3	5 May – 24 May 2013	28ºN	ra	~20 cm/s
4	25 May – 10 Jun 2013	**25ºN**	**d**	**>50 cm/s**
5	15 Jun – 4 Jul 2013	**24.5ºN**	**d**	**>70 cm/s**
6	5 Jul – 16 Jul 2013	27ºN	ra	<40 cm/s
7	3 Aug – 27 Aug 2013	28ºN	A	~20 cm/s
8	28 Aug – 5 Sep 2013	**25ºN**	**d**	**>60 cm/s**

9	6 Sep – 30 Sep 2013	26.5^{o}N	A	~20 cm/s
10	15 Nov – 31 Dec 2013	28^{o}N	A	<20 cm/s
11	1 Jul – 27 Jul 2014	**25.5^{o}N**	**d**	**>50 cm/s**
12	29 Jul – 30 Aug 2014	28.5^{o}N	ra	<20 cm/s
13	20 Sep – 4 Oct 2014	**25^{o}N**	**d**	**>40 cm/s**

Figure captions

Figure 1 (a) Gulf of Mexico (GoM) topography with the FKEYS-HYCOM model region indicated with a black box (simulations 2012-2016) and a white box (simulations 2009-2011); sections S1, S3 are indicated with solid black lines and the PKYF1 National Data Buoy Center buoy is marked with a black star. (b) Detail over an area marked with red box in (a); moorings region over the Pulley Ridge (PR), North Dry Tortugas (NDT) and South Dry Tortugas (SDT) areas; black cross marks indicate the positions of PR, NDT and SDT buoys over the Southwest Florida Shelf; section S2 is marked with a solid black line; the H1 location over the shelf-break (used in Figure 17) is marked with a cross; the 40 m, 60 m, 80 m, 100 m, 200 m, 500 m, 1000 m and 1500 m isobaths are indicated with solid white contours.

Figure 2 (a) Near-bottom temperature (^{o}C), derived from Pulley Ridge (PR), North (NDT) and South (SDT) Dry Tortugas mooring data (red lines) and FKEYS-HYCOM model simulation (black lines) for the observational period (08/2012-06/2015). (b) SST, derived from NDBC PKYF1 buoy (red line) and FKEYS-HYCOM (black line) and monthly averaged for the 2009-2016 period (the linear trends and the respective Sen's Slopes are shown). The temporal mean temperature, the Pearson correlation coefficient (r_c), and the Root Mean Square Error (*RMSE*) for each comparison are also given.

Figure 3 Sea Surface Temperature (SST, ^{o}C), derived from GHRSST (red line) and FKEYS-HYCOM (black line) (a) averaged over the model domain for the 2009-2016 period and (b) at Pulley Ridge (PR), North (NDT) and South (SDT) Dry Tortugas

moorings. The temporal mean temperature, the Pearson correlation coefficient (r_c), and the Root Mean Square Error (*RMSE*) for each comparison are also given.

Figure 4 Vectors of near-surface currents (cm/s) at Pulley Ridge (PR), North (NDT) and South (SDT) Dry Tortugas sites for the period 2013-2014, as derived from mooring observations (lower) and FKEYS-HYCOM simulations (upper).

Figure 5 Same as Figure 3 for near-bottom currents.

Figure 6 Comparison of monthly Kinetic Energy (KE) of vertically averaged currents between the FKEYS-HYCOM simulation and the respective measured currents at Pulley Ridge (PR; blue), North (NDT; black) and South (SDT; red) Dry Tortugas stations for the period 2012-2015. The linear fit (solid lines), the coefficient of determination (R^2), the Pearson correlation (r_c), the p-values ($p_{95\%}$) and the mean values of each location are also presented with the respective colors. The months of high KE are also indicated.

Figure 7 (a) Evolution of the eastward extension of Loop Current (LC) along the S1 section, as derived from AVISO Maps of Dynamic Topography (black dots) and GoM-HYCOM simulations (grey dots); S1 is marked in Figure 1a. (b) Kinetic energy (KE, cm^2s^{-2}) of vertically averaged currents, as derived from FKEYS-HYCOM simulations (blue line) and ADCP measurements (red line) at the PR location. The correlation coefficients between KE and LC extension are presented. The 5^{th} polynomial fits for the LC time series are also shown.

Figure 8 Daily location (latitude) of the Florida Current (FC) frontal position (red line, calculated from the FKEYS-HYCOM model as the position of the 20^{o}C isotherm at 150 m along the 83.5^{o}W meridian) and evolution of integrated Q_{S2} transport (Sv) across

section S2 (black line) for (a) 2012, (b) 2013, (c) 2014 and (d) 2015; S2 is marked in Figure 1b. Q_{S2} is positive (negative) for onshore (offshore) flow. The correlation coefficients between the two time series and the mean FC latitude (FC_{mean}) for each year over the 2012-2015 4-year period are also presented. Groups discussed in Figure 9 are indicated with x symbols and dashed lines (blue: Group 1; red: Group 2).

Figure 9 Model-computed wind-stress (N/m^2), derived from COAMPS and NAVGEM, Sea Surface Height (SSH, cm) and near-surface current vectors (m/s), derived from the FKEYS-HYCOM simulation, zooming around the Southwest Florida Shelf on (a) 6 June 2013, (b) 19 July 2014, (c) 30 March 2014, and (d) 18 August 2014. Currents and winds are plotted every 20 grid points. The positions of Pulley Ridge (PR), North (NDT) and South (SDT) Dry Tortugas buoys over the Southwest Florida Shelf are marked and the 100 m isobath is indicated with a solid contour line.

Figure 10 Snapshots of model-computed near surface currents ($m\ s^{-1}$, upper panels) and Sea Surface Height (SSH, cm, lower panels) derived from the FKEYS-HYCOM simulation, zooming around the Southwest Florida Shelf, with superimposed NOAA/AOML drifter trajectories (dots along track at 24 hour interval) deployed in North (NDT; grey or red track) and South (SDT; black or white track) Dry Tortugas on 24 August 2013 and 22 August 2013, respectively. The position of each drifter is indicated on the respective snapshot: (a) 1 September 2013, (b) 6 September 2013, (c) 13 September 2013, (d) 1 October 2013, (e) 10 October 2013 and (f) 15 October 2013. The color scale of currents is reflected on the vector colors. The different drifter speeds along each trajectory are indicated by colored dots (scale within the box insert in the upper left

panel). The positions of Pulley Ridge (PR), NDT and SDT buoys over the Southwest Florida Shelf are marked.

Figure 11 Rose diagrams in the North Dry Tortugas (NDT, left) and Pulley Ridge (PR, right) locations for: (upper panels) winds derived by COAMPS atmospheric fields, vertically averaged currents derived by (middle panels) ADCP measurements and (lower panels) FKEYS-HYCOM simulations. The % of frequency of occurrence is provided for four directions at the bottom of each rose diagram (toward NE, SE, SW, NW).

Figure 12 Evolution of vertically averaged current velocity as derived from ADCP measurements (dots) and from the FKEYS-HYCOM simulation (lines) at the Pulley Ridge (PR) mooring location for (a) 2013 and (b) 2014. Thirteen characteristic connectivity events between regional and local circulation (see Table 2 for exact dates) are indicated with triangles. Four events discussed in Figure 13 are marked in color (E5: red, E7: blue, E11: green, E12: cyan). The vertical solid (dashed) lines mark selected dates associated with these four events, shown in the Figure 13 right (left) panels.

Figure 13 Sea Surface Height (SSH) distribution as derived from GoM-HYCOM simulations for Events 5, 7, 11 and 12 (Table 2 and Figure 12). The locations of the major cyclonic (C1, C2, C3, C4, C5, C6) and anticyclonic circulation patterns (Loop Current Eddy: LCE, Anticyclonic eddies along the West Florida Shelf slope: A1, A2) during each event are also presented.

Figure 14 Spatial distribution of (top to bottom) AVISO Sea Level Anomaly (SLA), GoM-HYCOM Sea Surface Height (SSH), GHRSST Sea Surface Temperature (SST), and GoM-HYCOM SST on 22 November 2013 (left panels) and 6 December 2013 (right panels), during event E10 (Figure 12 and Table 2). The FKEYS-HYCOM region is

indicated with a black box. Red dots indicate the positions of Pulley Ridge (PR), Northern Dry Tortugas (NDT), and Southern Dry Tortugas (SDT) buoys over the Southwest Florida Shelf. The Loop Current Eddy (LCE), the anticyclonic eddies (A3, A4), the major cyclonic eddy (C) and the 26^{o}C isotherm are marked.

Figure 15 Model-computed near-surface current vectors (m/s), derived from the GoM-HYCOM simulation, zooming over the Southeastern GoM and the Straits of Florida on (a) 22 November 2013 and (b) 6 December 2013 (event E10, Figure 12 and Table 2) (upper panels). Respective maps of bottom temperature difference (dT_{bottom}, ^{o}C) between (c) 22 November and 1 November and between (d) 6 December and 22 November (lower panels). Currents are plotted every 6 grid points and vectors below 0.1 m/s are not included. The positions of Pulley Ridge (PR), North (NDT) and South (SDT) Dry Tortugas buoys over the Southwest Florida Shelf are also marked and the 100 m isobath is indicated with a solid contour line. The Loop Current (LC), the anticyclonic eddies (A3, A4) and the major cyclonic eddy (C), shown in Figure 14, are marked.

Figure 16 (a) Monthly stratification frequency (N, sec^{-1}) with (seasonality included, black line) and without (seasonal adjusted values, red line) the seasonal cycle at the Pulley Ridge (PR) mooring location for the 2012-2015 period, as derived from the FKEYS-HYCOM model simulation, and the respective evolution of the mean monthly eastward LC extension along the S1 section (black dots), as derived from observations (AVISO). Two periods with strong and zero LC influence are marked; they correspond to Events E8 and E12, respectively (Figure 12 and Table 2). (b) Vertical distribution of temperature and zonal currents (positive: eastward; negative: westward) along the S3

Section over the upper 300 m during events E8 (left) and E12 (right). S1 and S3 are marked in Figure 1a.

Figure 17 Hovmöller diagrams of (a) temperature (^{o}C) and (b) vertical velocity during 2012-2015 over the upper 100 m at the H1 location (Figure 1b), as derived by the FKEYS-HYCOM simulation. Two periods with strong and zero Loop Current (LC) influence are marked; they correspond to Events E8 and E12, respectively (Figure 12 and Table 2).

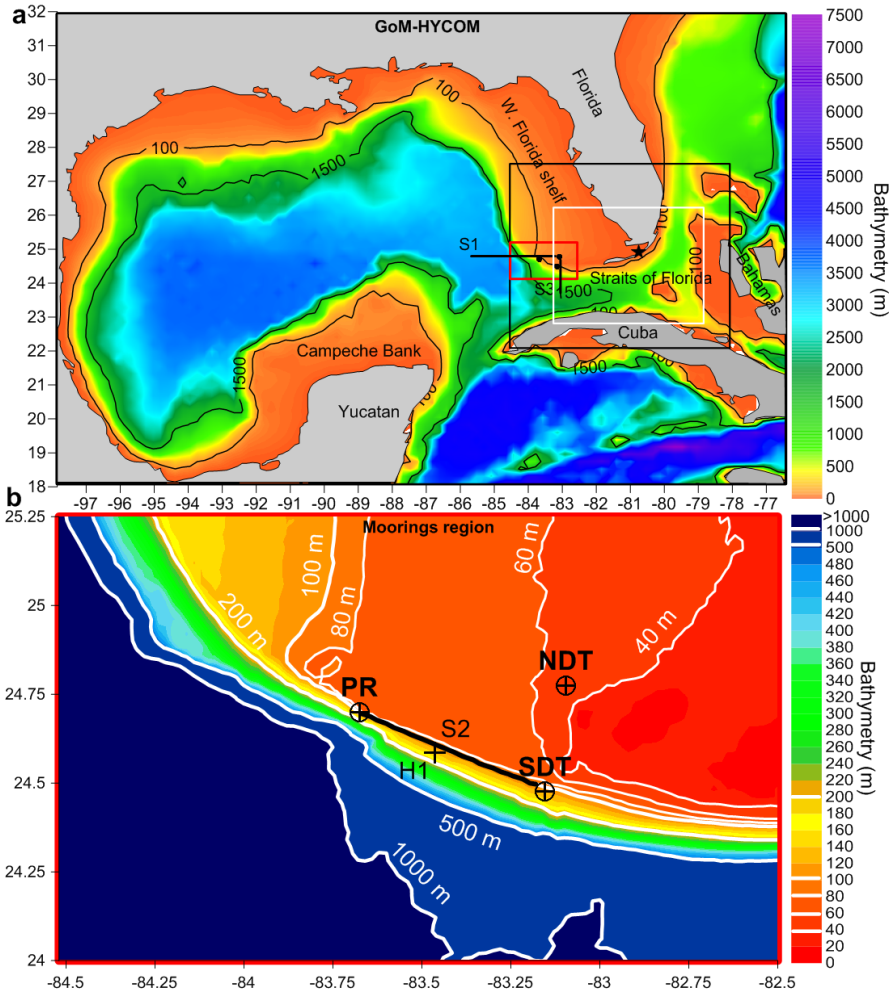

Figure 1 (a) Gulf of Mexico (GoM) topography with the FKEYS-HYCOM model region indicated with a black box (simulations 2012-2016) and a white box (simulations 2009-2011); sections S1, S3 are indicated with solid black lines and the PKYF1 National Data Buoy Center buoy is marked with a black star. (b) Detail over an area marked with red box in (a); moorings region over the Pulley Ridge (PR), North Dry Tortugas (NDT) and South Dry Tortugas (SDT) areas; black cross marks indicate the positions of PR, NDT and SDT buoys over the Southwest Florida Shelf; section S2 is marked with a solid black line; the H1 location over the shelf-break (used in Figure 17) is marked with a cross; the 40 m, 60 m, 80 m, 100 m, 200 m, 500 m, 1000 m and 1500 m isobaths are indicated with solid white contours.

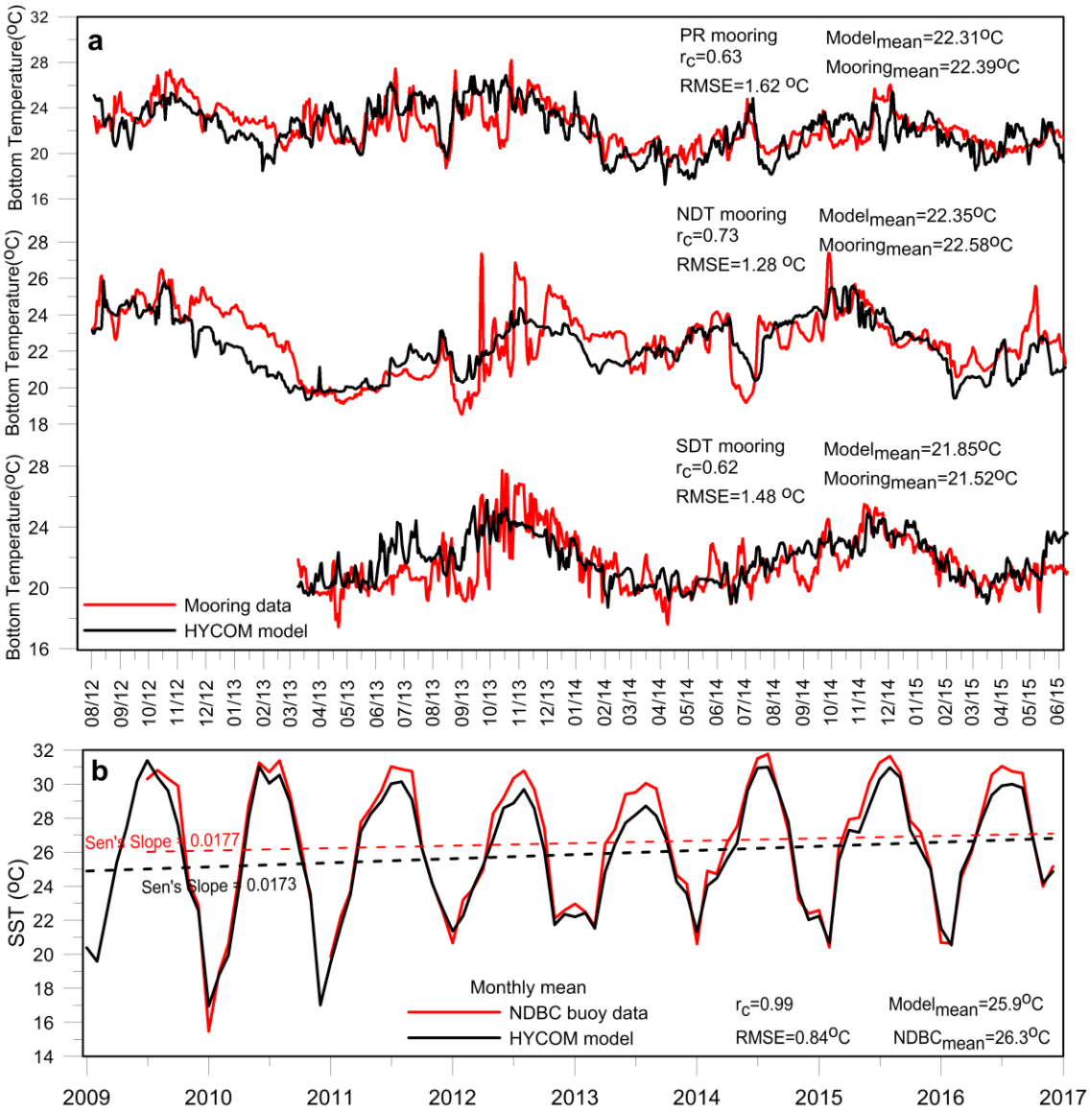

Figure 2 (a) Near-bottom temperature (°C), derived from Pulley Ridge (PR), North (NDT) and South (SDT) Dry Tortugas mooring data (red lines) and FKEYS-HYCOM model simulation (black lines) for the observational period (08/2012-06/2015). (b) SST, derived from NDBC PKYF1 buoy (red line) and FKEYS-HYCOM (black line) and monthly averaged for the 2009-2016 period (the linear trends and the respective Sen's Slopes are shown). The temporal mean temperature, the Pearson correlation coefficient (r_c), and the Root Mean Square Error (*RMSE*) for each comparison are also given.

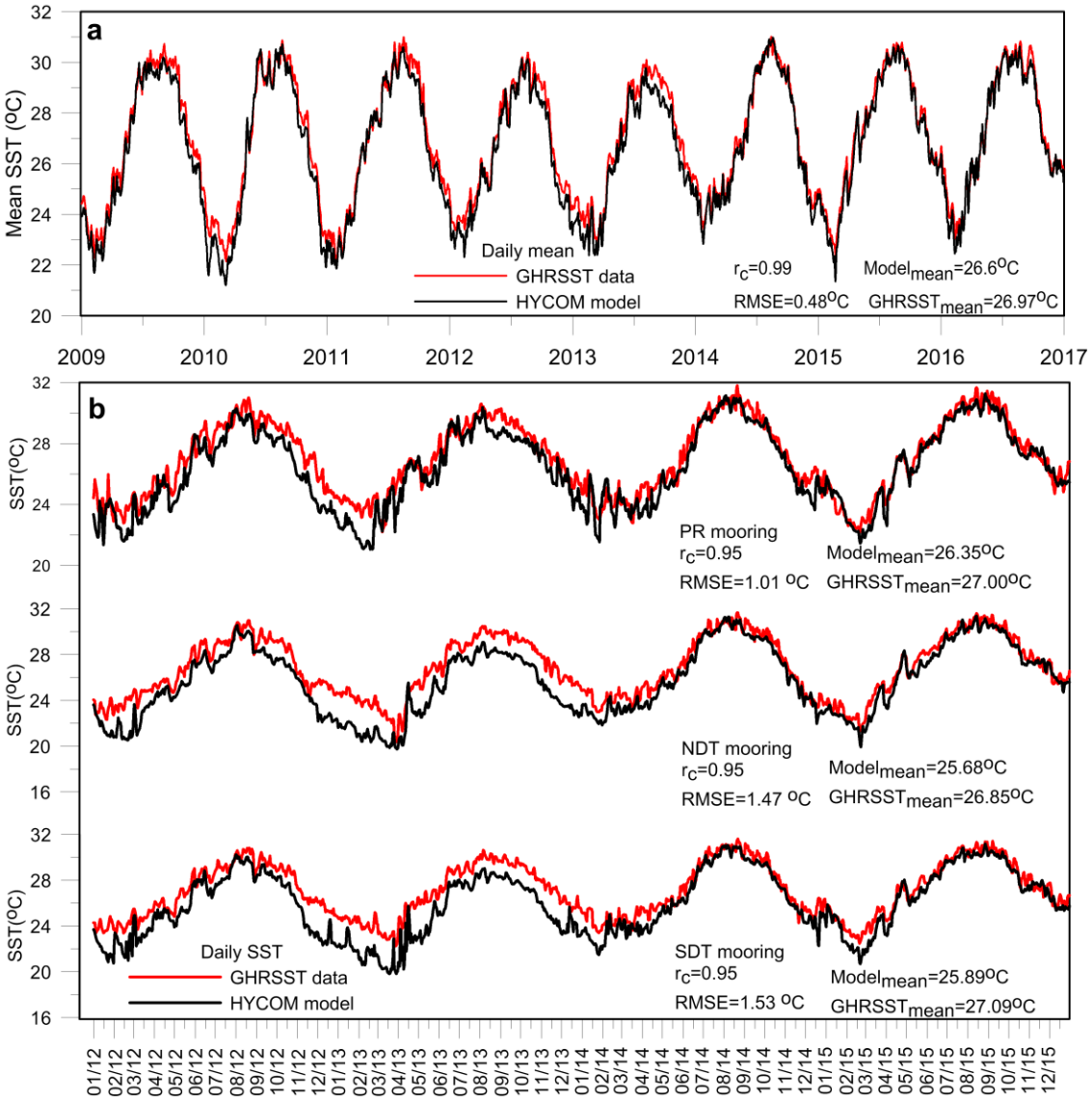

Figure 3 Sea Surface Temperature (SST, °C), derived from GHRSST (red line) and FKEYS-HYCOM (black line) (a) averaged over the model domain for the 2009-2016 period and (b) at Pulley Ridge (PR), North (NDT) and South (SDT) Dry Tortugas moorings. The temporal mean temperature, the Pearson correlation coefficient (r_c), and the Root Mean Square Error (*RMSE*) for each comparison are also given.

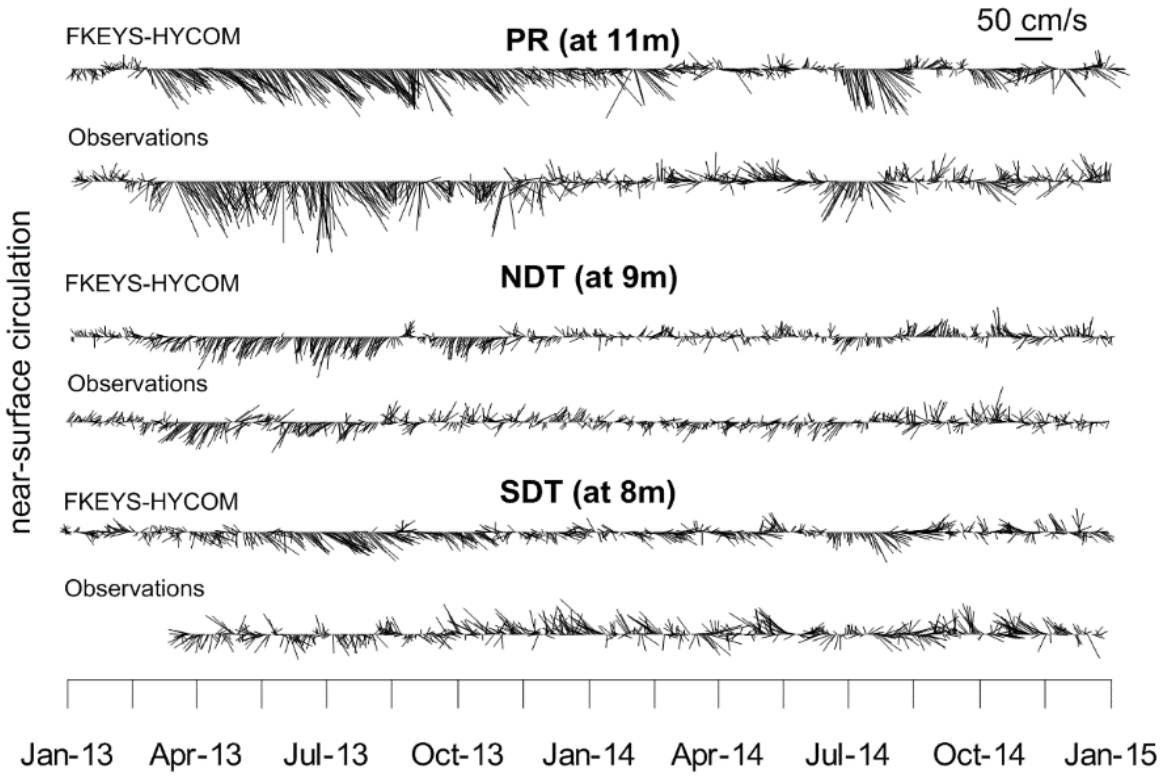

Figure 4 Vectors of near-surface currents (cm/s) at Pulley Ridge (PR), North (NDT) and South (SDT) Dry Tortugas sites for the period 2013-2014, as derived from mooring observations (lower) and FKEYS-HYCOM simulations (upper).

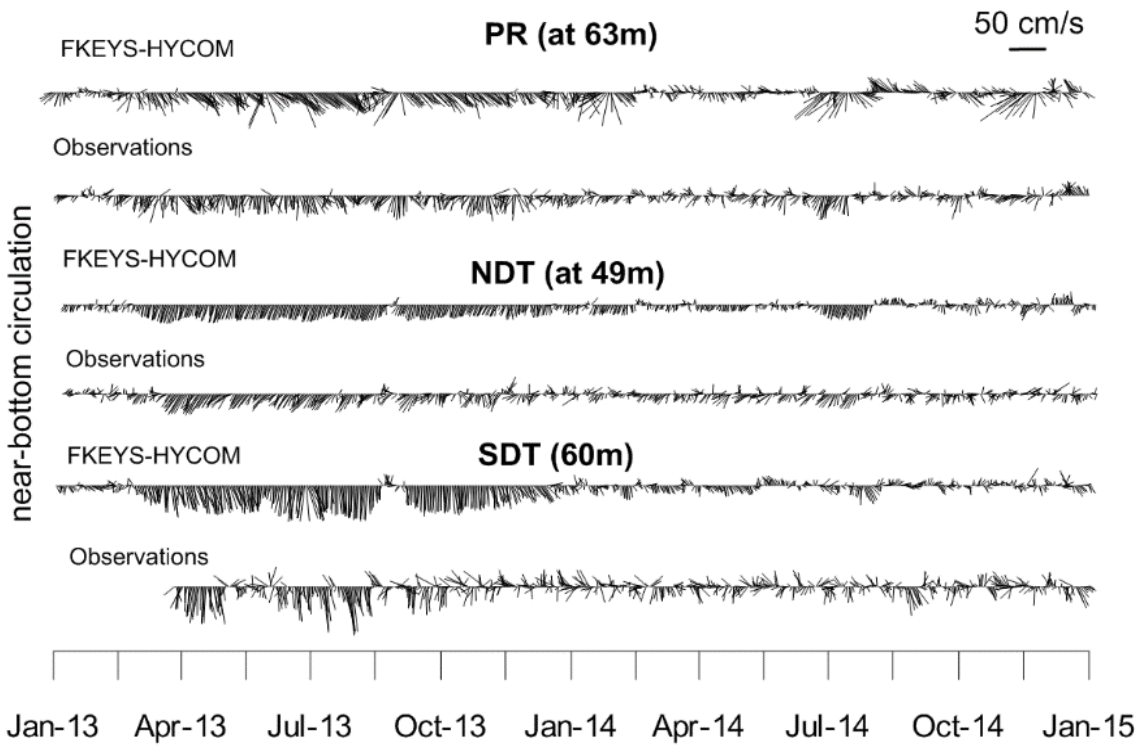

Figure 5 Same as Figure 4 for near-bottom currents.

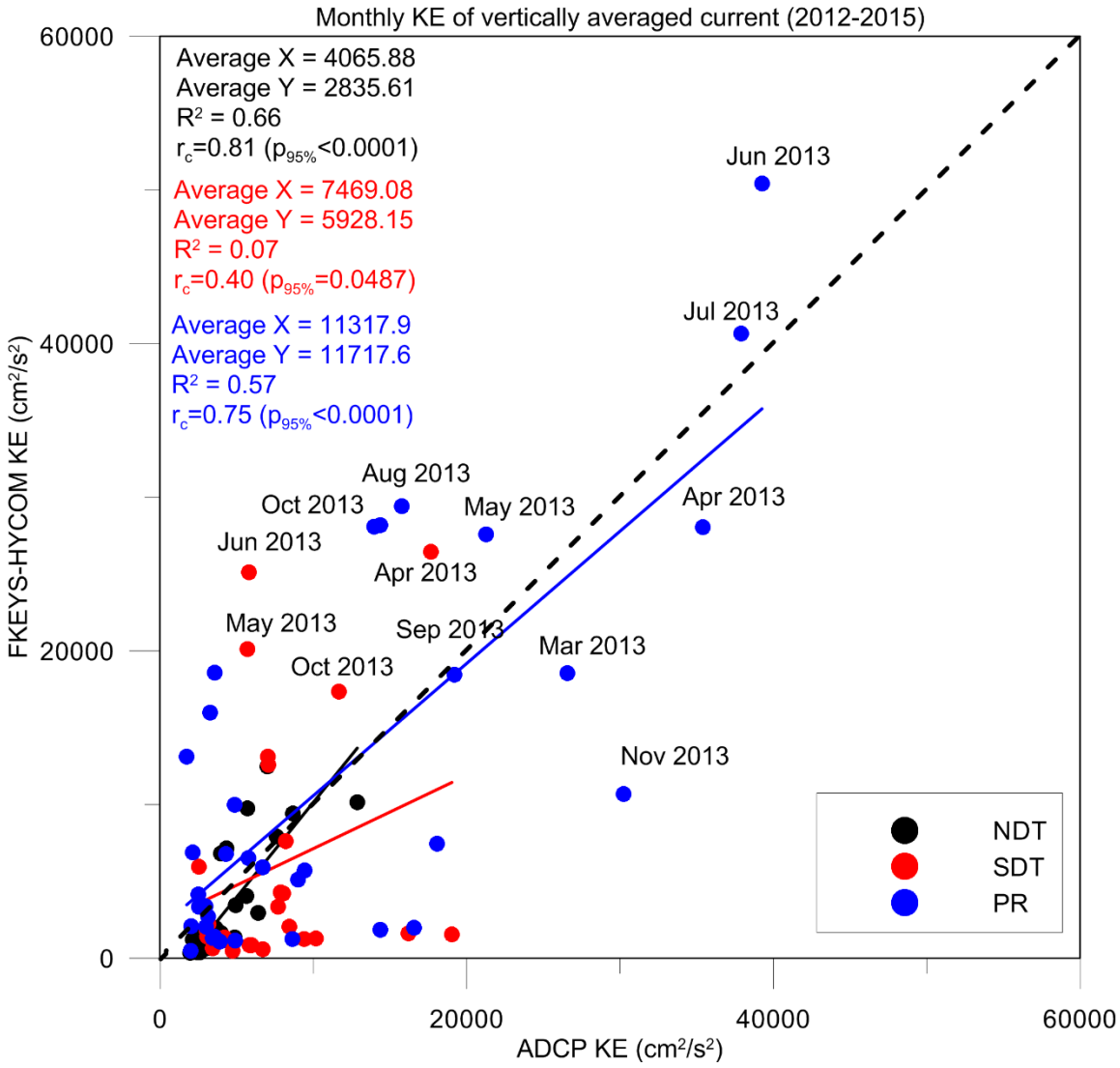

Figure 6 Comparison of monthly Kinetic Energy (KE) of vertically averaged currents between the FKEYS-HYCOM simulation and the respective measured currents at Pulley Ridge (PR; blue), North (NDT; black) and South (SDT; red) Dry Tortugas stations for the period 2012-2015. The linear fit (solid lines), the coefficient of determination (R^2), the Pearson correlation (r_c), the p-values ($p_{95\%}$) and the mean values of each location are also presented with the respective colors. The months of high KE are also indicated.

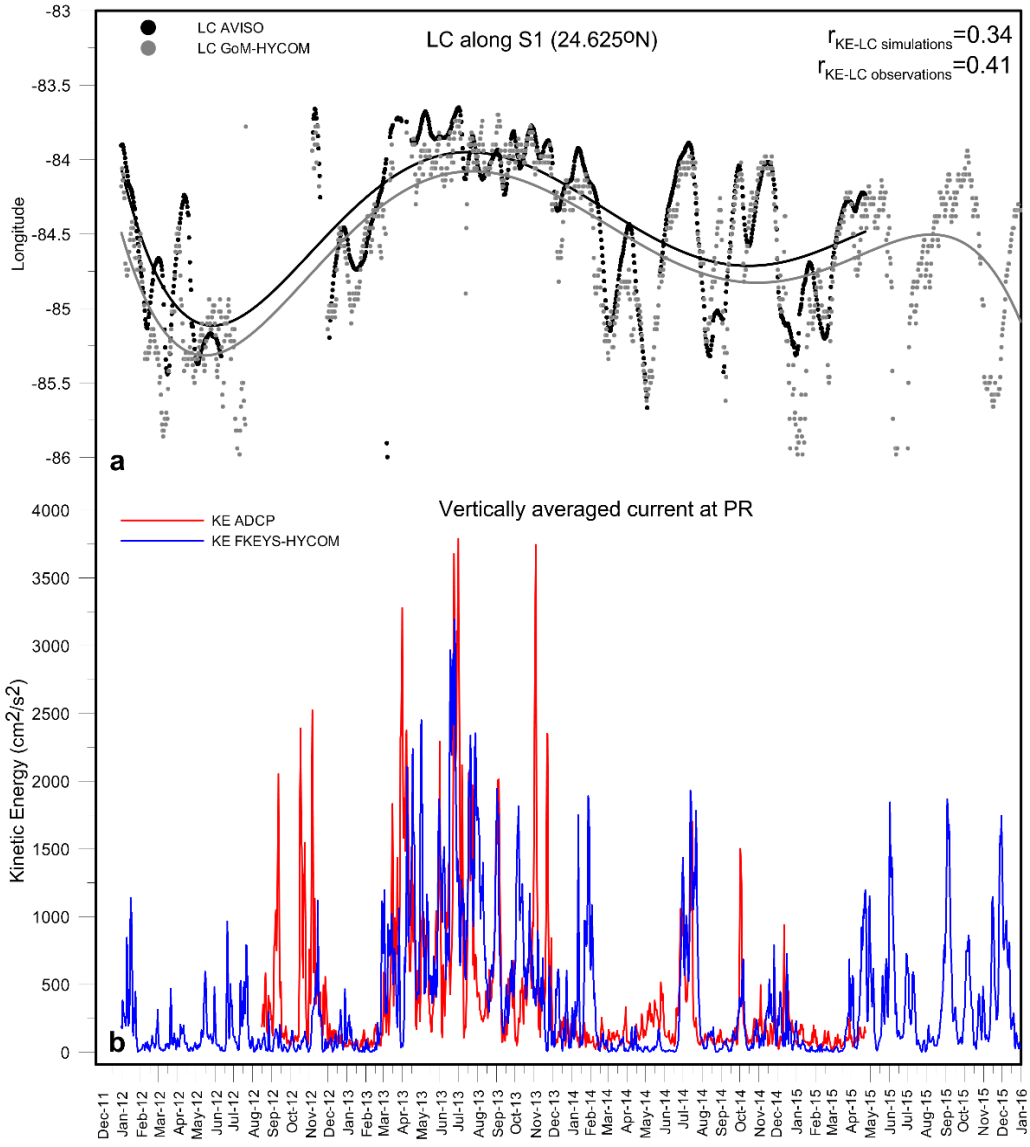

Figure 7 (a) Evolution of the eastward extension of Loop Current (LC) along the S1 section, as derived from AVISO Maps of Dynamic Topography (black dots) and GoM-HYCOM simulations (grey dots); S1 is marked in Figure 1a. (b) Kinetic energy (KE, cm^2s^{-2}) of vertically averaged currents, as derived from FKEYS-HYCOM simulations (blue line) and ADCP measurements (red line) at the PR location. The correlation coefficients between KE and LC extension are presented. The 5^{th} polynomial fits for the LC time series are also shown.

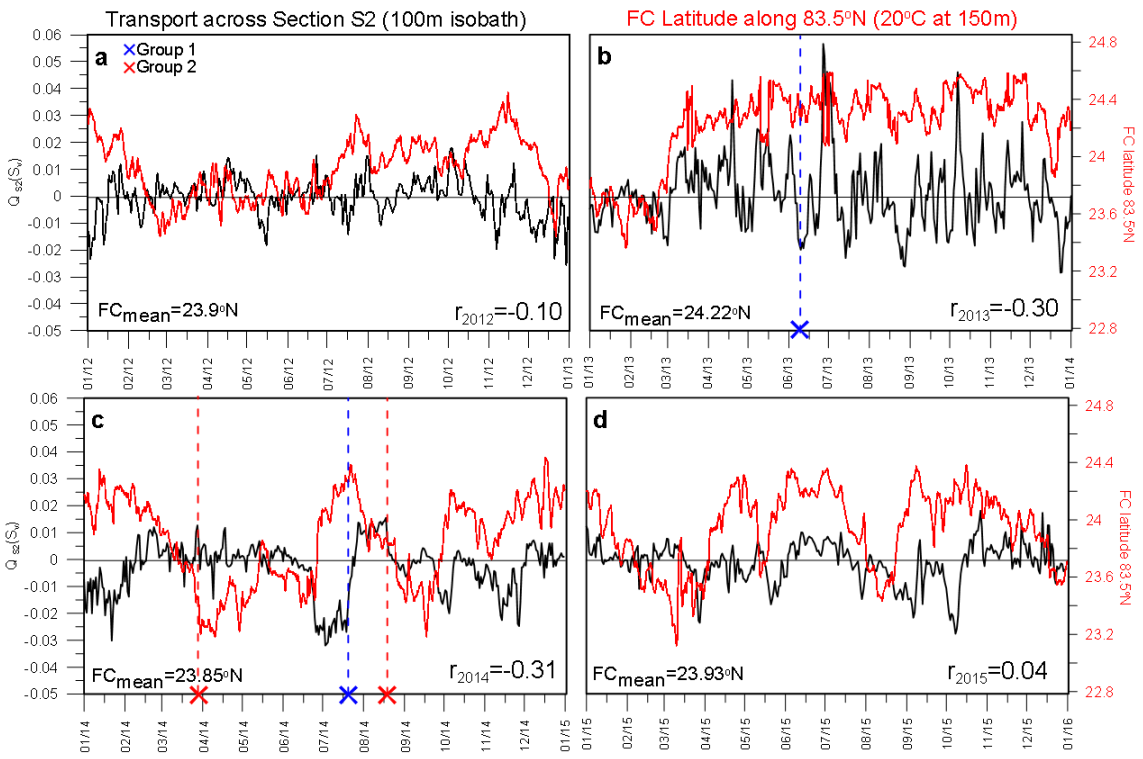

Figure 8 Daily location (latitude) of the Florida Current (FC) frontal position (red line, calculated from the FKEYS-HYCOM model as the position of the 20ºC isotherm at 150 m along the 83.5ºW meridian) and evolution of integrated Q_{S2} transport (Sv) across section S2 (black line) for (a) 2012, (b) 2013, (c) 2014 and (d) 2015; S2 is marked in Figure 1b. Q_{S2} is positive (negative) for onshore (offshore) flow. The correlation coefficients between the two time series and the mean FC latitude (FC_{mean}) for each year over the 2012-2015 4-year period are also presented. Groups discussed in Figure 9 are indicated with x symbols and dashed lines (blue: Group 1; red: Group 2).

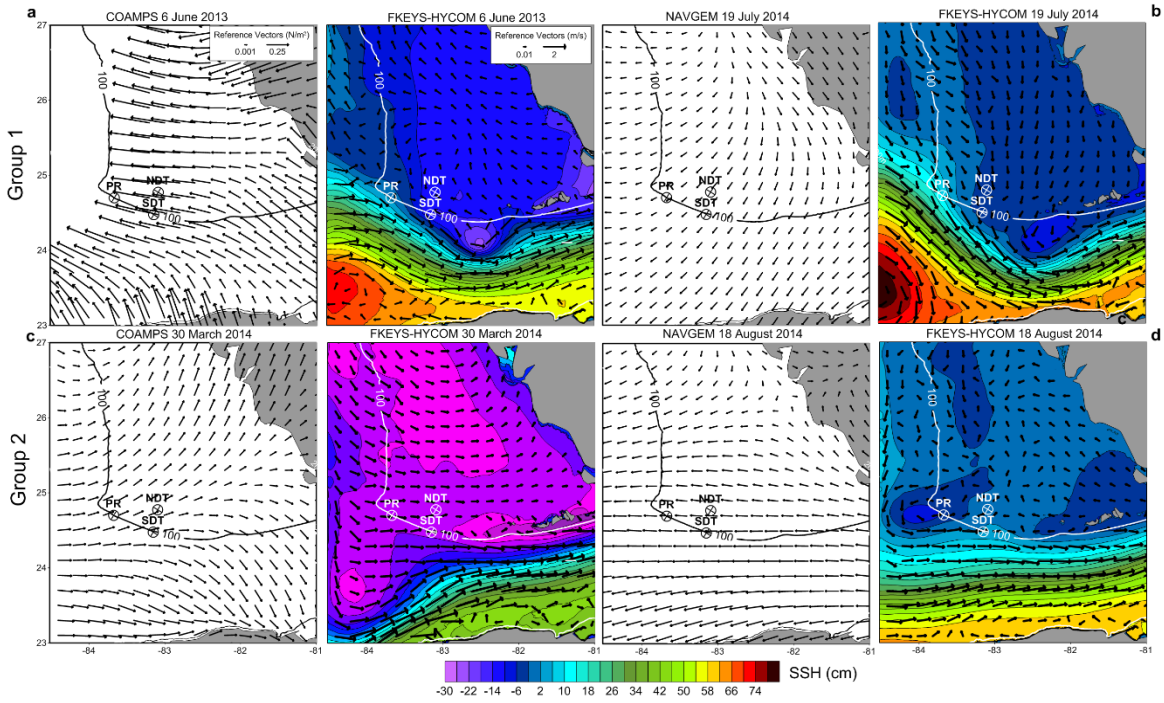

Figure 9 Model-computed wind-stress (N/m^2), derived from COAMPS and NAVGEM, Sea Surface Height (SSH, cm) and near-surface current vectors (m/s), derived from the FKEYS-HYCOM simulation, zooming around the Southwest Florida Shelf on (a) 6 June 2013, (b) 19 July 2014, (c) 30 March 2014, and (d) 18 August 2014. Currents and winds are plotted every 20 grid points. The positions of Pulley Ridge (PR), North (NDT) and South (SDT) Dry Tortugas buoys over the Southwest Florida Shelf are marked and the 100 m isobath is indicated with a solid contour line.

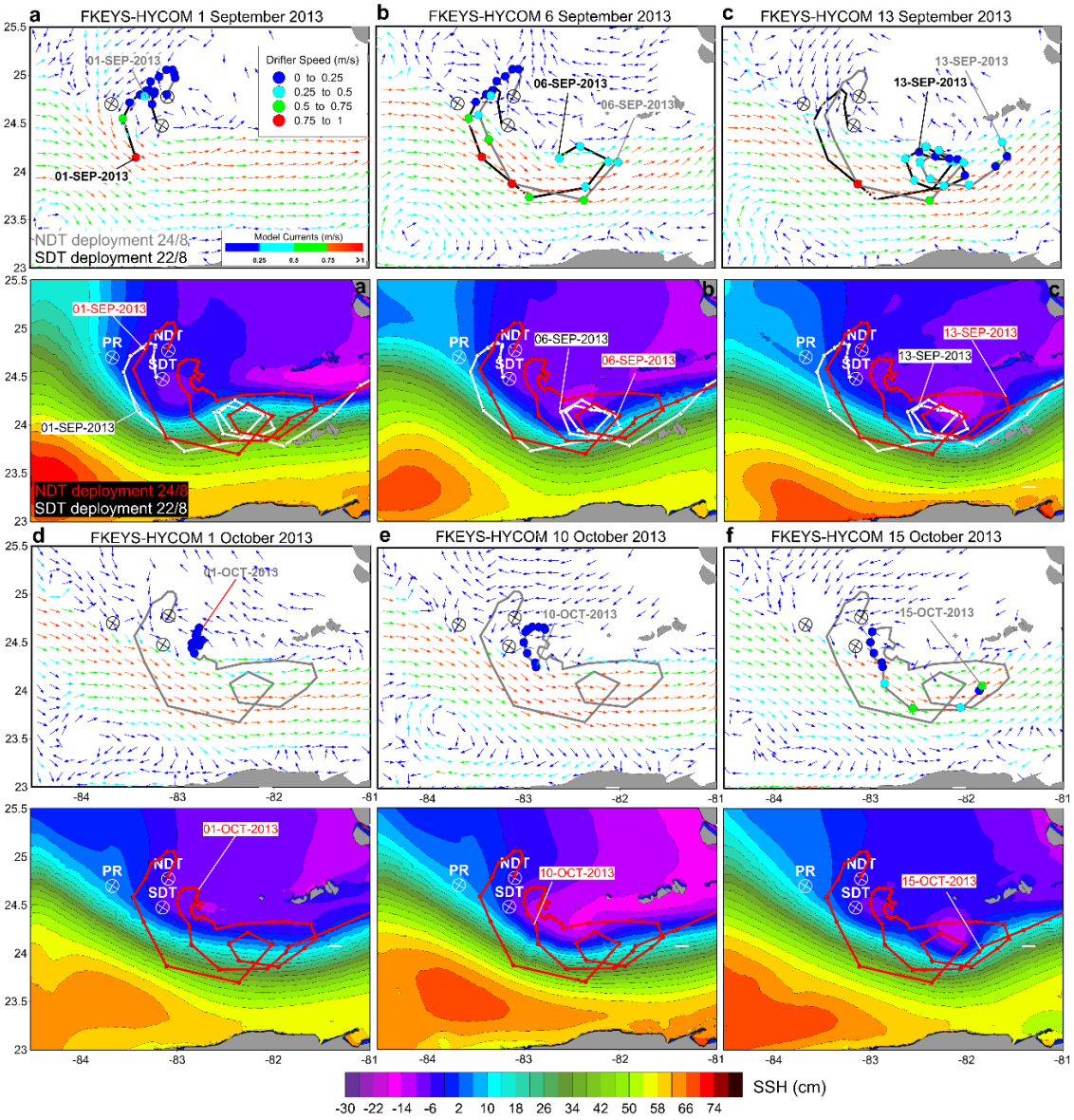

Figure 10 Snapshots of model-computed near surface currents (m s^{-1}, upper panels) and Sea Surface Height (SSH, cm, lower panels) derived from the FKEYS-HYCOM simulation, zooming around the Southwest Florida Shelf, with superimposed NOAA/AOML drifter trajectories (dots along track at 24 hour interval) deployed in North (NDT; grey or red track) and South (SDT; black or white track) Dry Tortugas on 24 August 2013 and 22 August 2013, respectively. The position of each drifter is indicated on the respective snapshot: (a) 1 September 2013, (b) 6 September 2013, (c) 13 September 2013, (d) 1 October 2013, (e) 10 October 2013 and (f) 15 October 2013. The color scale of currents is reflected on the vector colors. The different drifter speeds along each trajectory are indicated by colored dots (scale within the box insert in the upper left panel). The positions of Pulley Ridge (PR), NDT and SDT buoys over the Southwest Florida Shelf are marked.

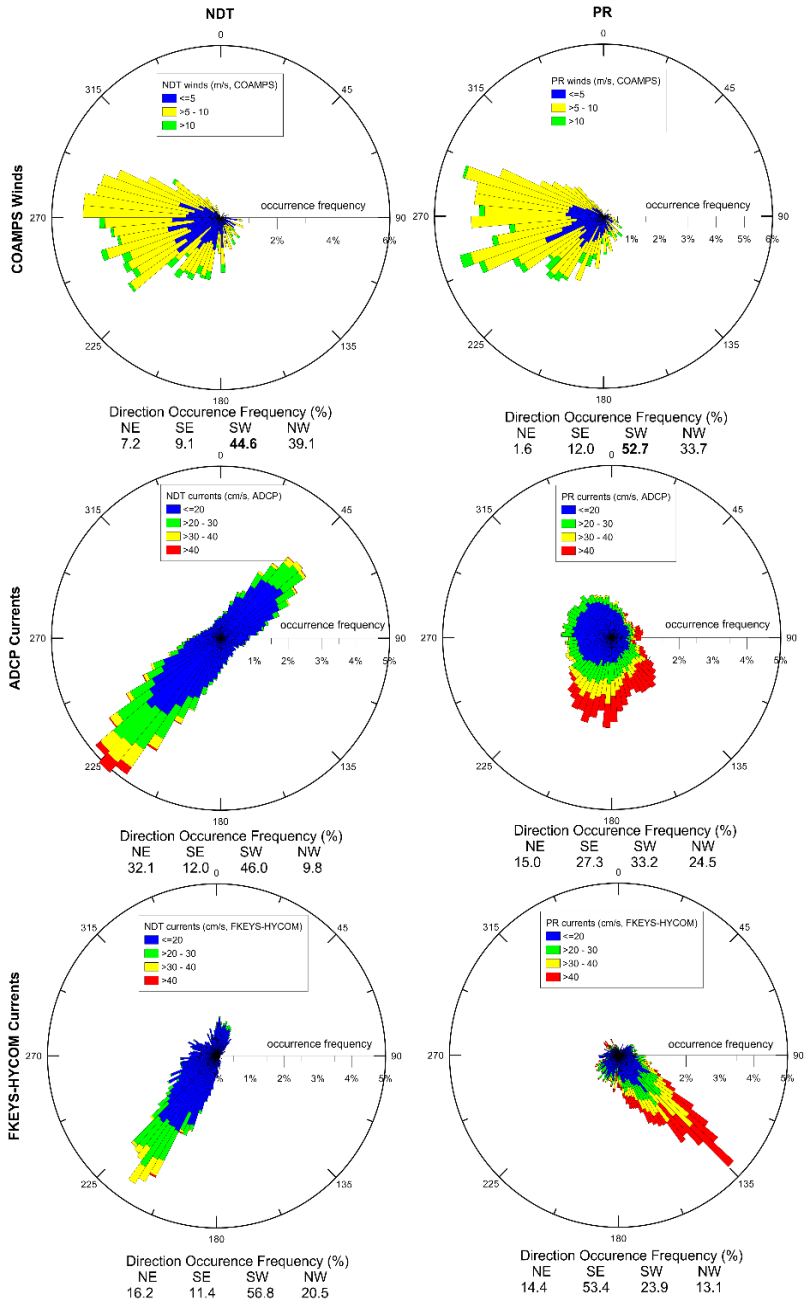

Figure 11 Rose diagrams in the North Dry Tortugas (NDT, left) and Pulley Ridge (PR, right) locations for: (upper panels) winds derived by COAMPS atmospheric fields, vertically averaged currents derived by (middle panels) ADCP measurements and (lower panels) FKEYS-HYCOM simulations. The % of frequency of occurrence is provided for four directions at the bottom of each rose diagram (toward NE, SE, SW, NW).

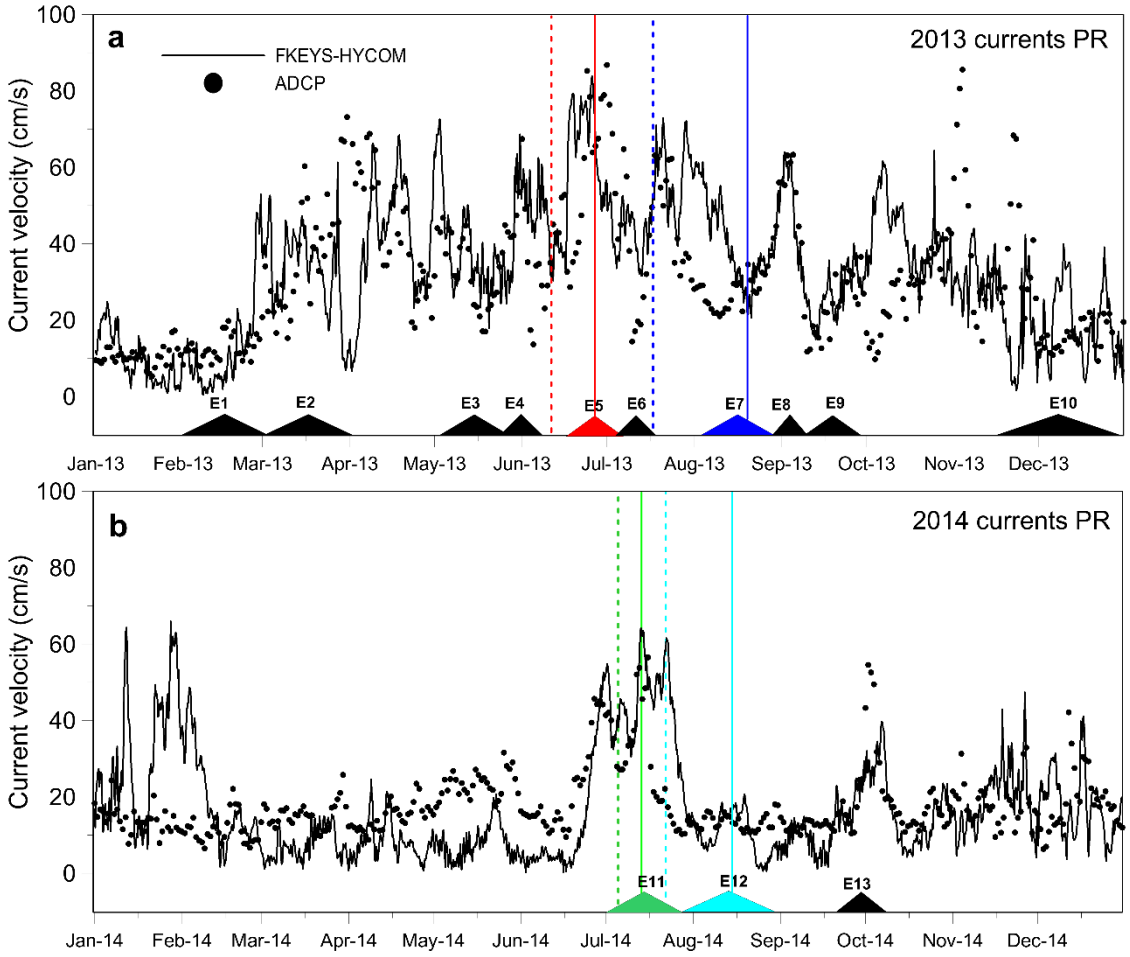

Figure 12 Evolution of vertically averaged current velocity as derived from ADCP measurements (dots) and from the FKEYS-HYCOM simulation (lines) at the Pulley Ridge (PR) mooring location for (a) 2013 and (b) 2014. Thirteen characteristic connectivity events between regional and local circulation (see Table 2 for exact dates) are indicated with triangles. Four events discussed in Figure 13 are marked in color (E5: red, E7: blue, E11: green, E12: cyan). The vertical solid (dashed) lines mark selected dates associated with these events, shown in the Figure 13 right (left) panels.

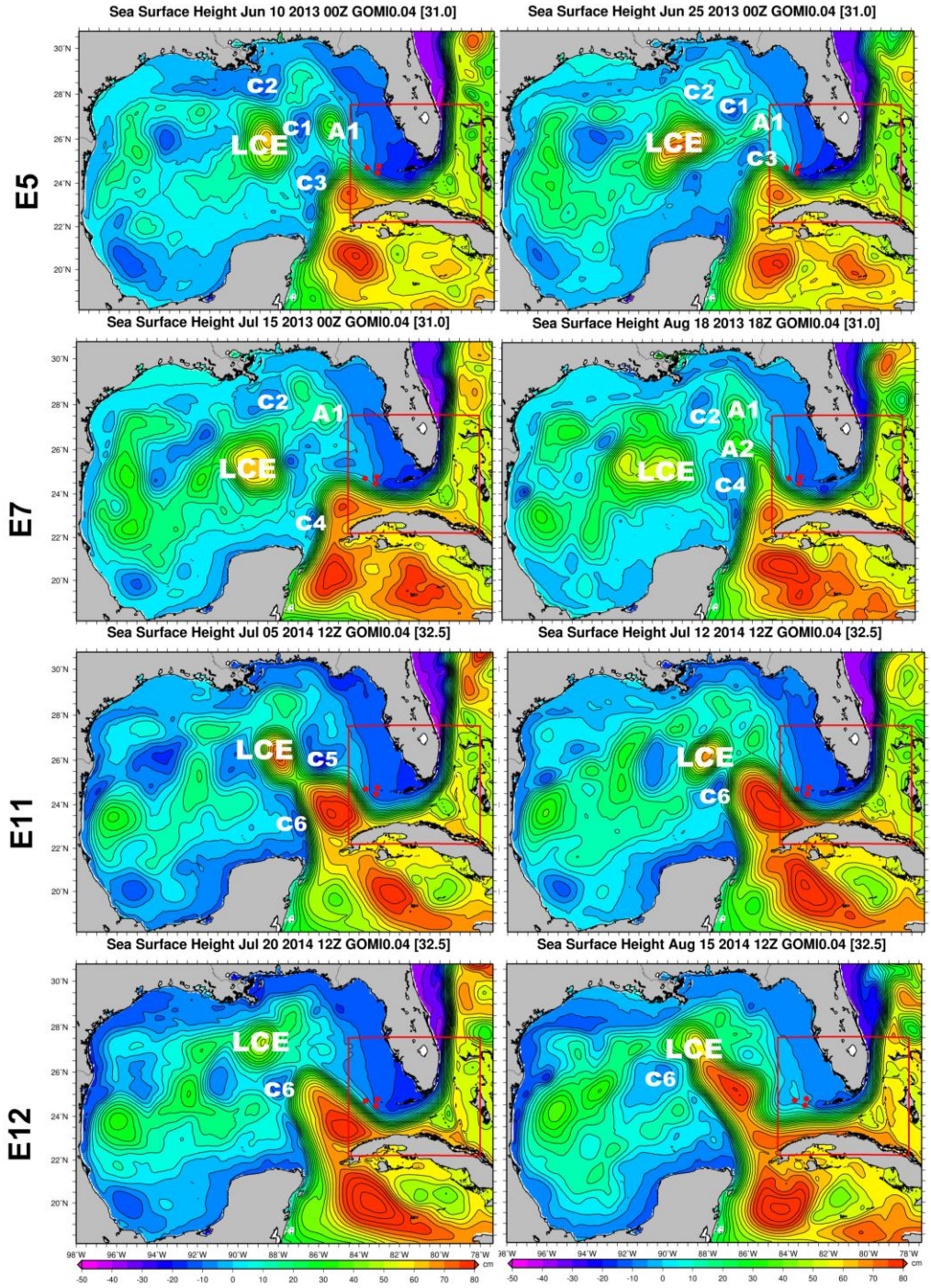

Figure 13 Sea Surface Height (SSH) distribution as derived from GoM-HYCOM simulations for Events 5, 7, 11 and 12 (Table 2 and Figure 12). The locations of the major cyclonic (C1, C2, C3, C4, C5, C6) and anticyclonic circulation patterns (Loop Current Eddy: LCE, Anticyclonic eddies along the West Florida Shelf slope: A1, A2) during each event are also presented.

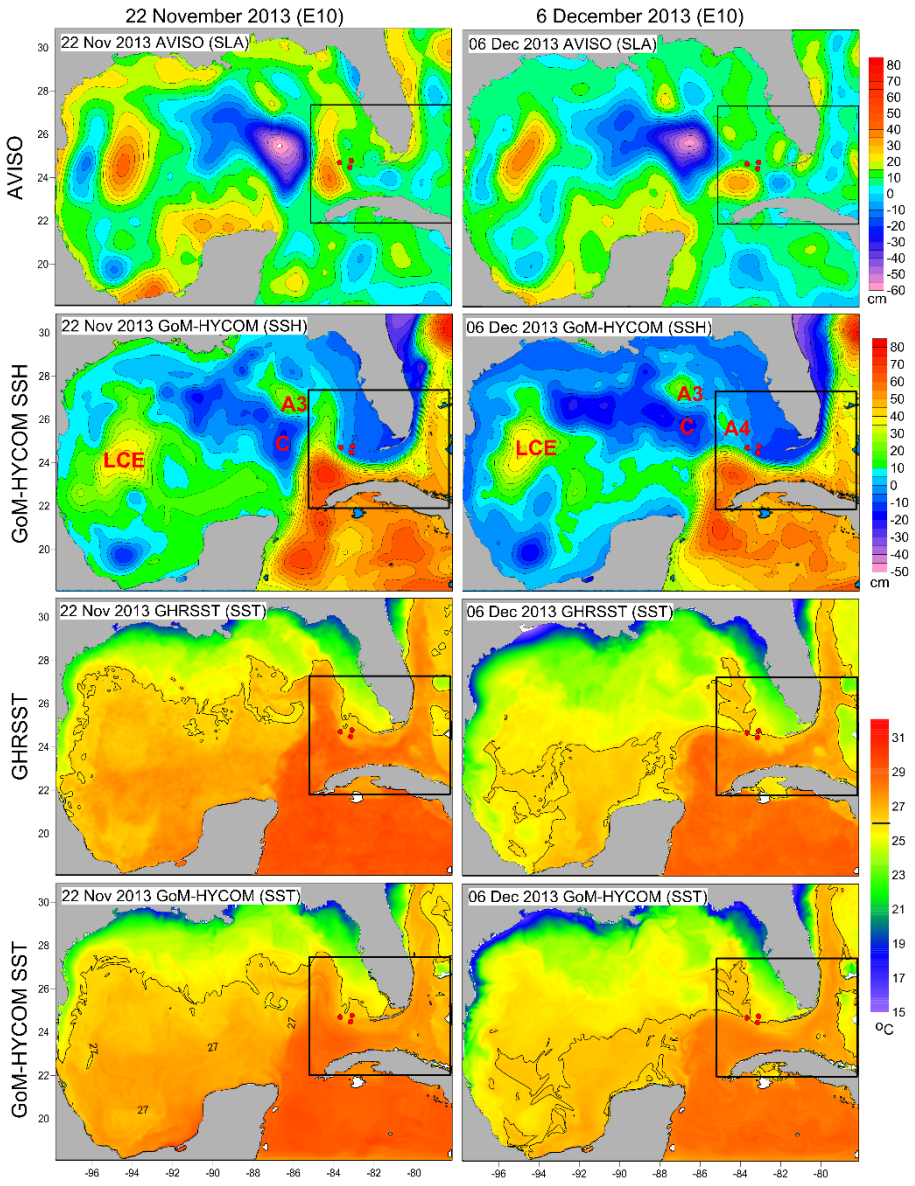

Figure 14 Spatial distribution of (top to bottom) AVISO Sea Level Anomaly (SLA), GoM-HYCOM Sea Surface Height (SSH), GHRSST Sea Surface Temperature (SST), and GoM-HYCOM SST on 22 November 2013 (left panels) and 6 December 2013 (right panels), during event E10 (Figure 12 and Table 2). The FKEYS-HYCOM region is indicated with a black box. Red dots indicate the positions of Pulley Ridge (PR), Northern Dry Tortugas (NDT), and Southern Dry Tortugas (SDT) buoys over the Southwest Florida Shelf. The Loop Current Eddy (LCE), the anticyclonic eddies (A3, A4), the major cyclonic eddy (C) and the 26°C isotherm are marked.

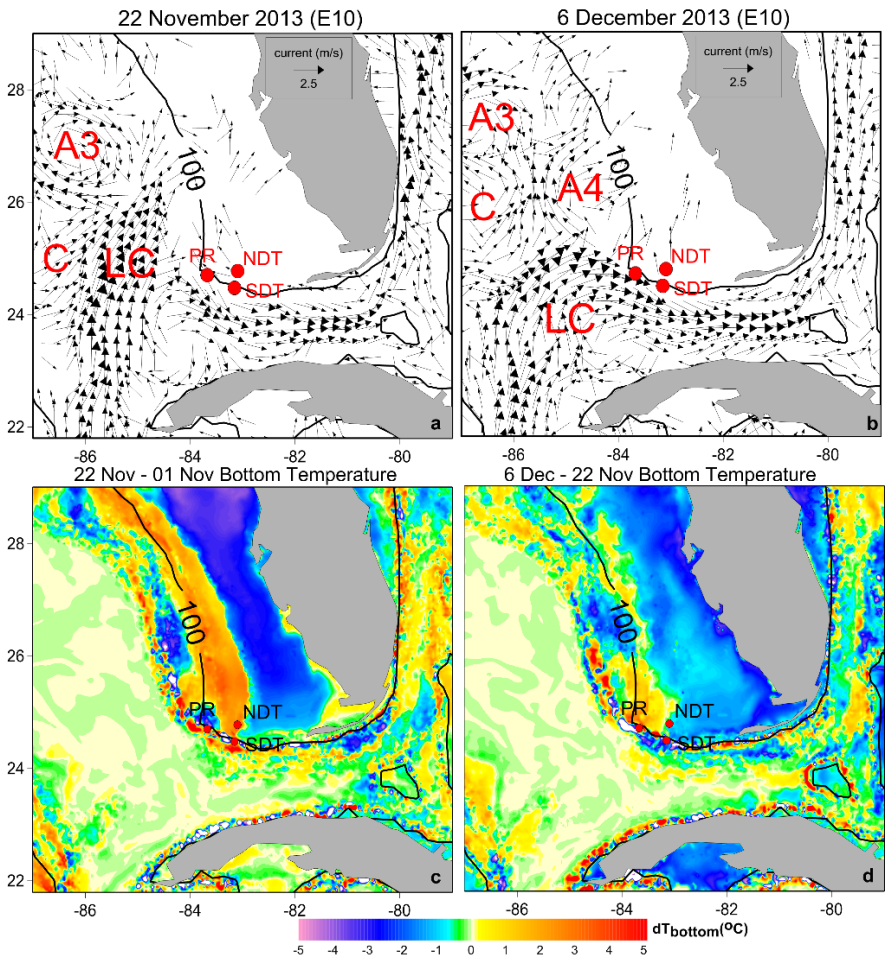

Figure 15 Model-computed near-surface current vectors (m/s), derived from the GoM-HYCOM simulation, zooming over the Southeastern GoM and the Straits of Florida on (a) 22 November 2013 and (b) 6 December 2013 (event E10, Figure 12 and Table 2) (upper panels). Respective maps of bottom temperature difference (dT_{bottom}, ^{o}C) between (c) 22 November and 1 November and between (d) 6 December and 22 November (lower panels). Currents are plotted every 6 grid points and vectors below 0.1 m/s are not included. The positions of Pulley Ridge (PR), North (NDT) and South (SDT) Dry Tortugas buoys over the Southwest Florida Shelf are also marked and the 100 m isobath is indicated with a solid contour line. The Loop Current (LC), the anticyclonic eddies (A3, A4) and the major cyclonic eddy (C), shown in Figure 14, are marked.

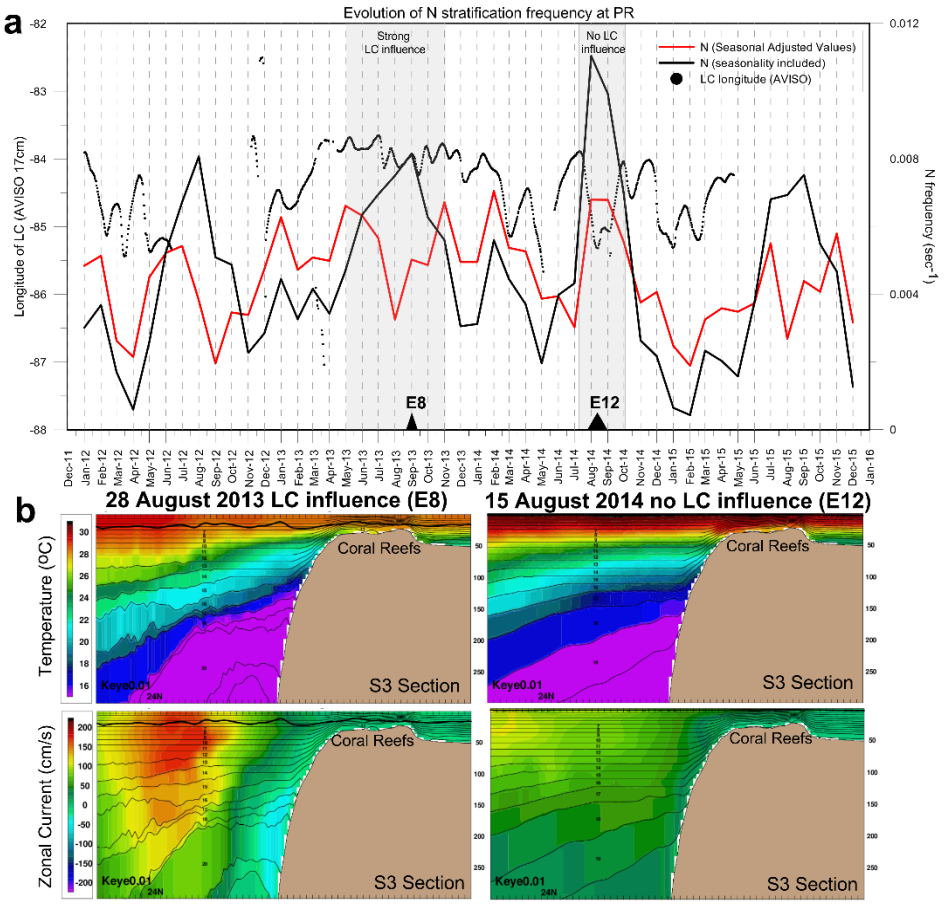

Figure 16 (a) Monthly stratification frequency (N, sec^{-1}) with (seasonality included, black line) and without (seasonal adjusted values, red line) the seasonal cycle at the Pulley Ridge (PR) mooring location for the 2012-2015 period, as derived from the FKEYS-HYCOM model simulation, and the respective evolution of the mean monthly eastward LC extension along the S1 section (black dots), as derived from observations (AVISO). Two periods with strong and zero LC influence are marked; they correspond to Events E8 and E12, respectively (Figure 12 and Table 2). (b) Vertical distribution of temperature and zonal currents (positive: eastward; negative: westward) along the S3 Section over the upper 300 m during events E8 (left) and E12 (right). S1 and S3 are marked in Figure 1a.

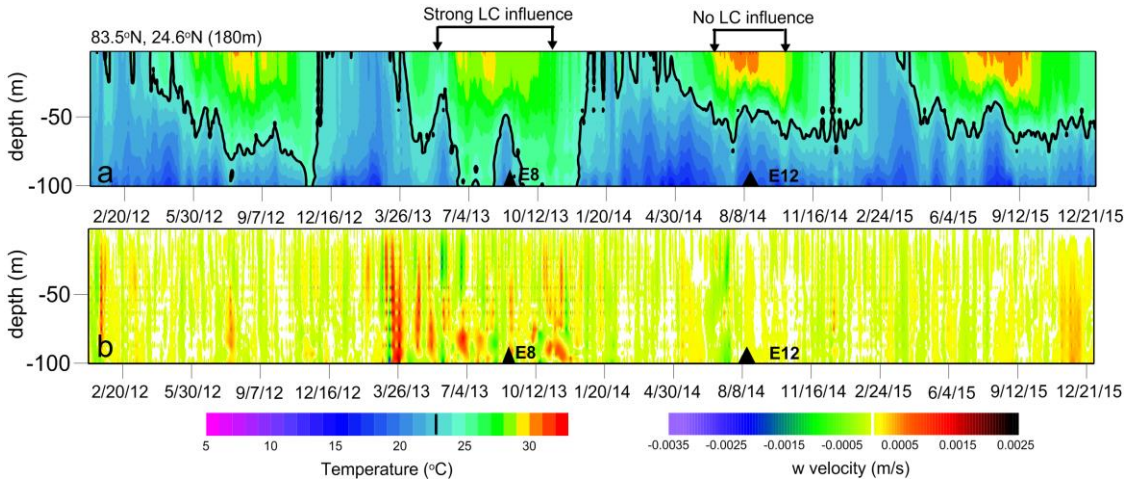

Figure 17 Hovmöller diagrams of (a) temperature (^{o}C) and (b) vertical velocity during 2012-2015 over the upper 100 m at the H1 location (Figure 1b), as derived by the FKEYS-HYCOM simulation. Two periods with strong and zero Loop Current (LC) influence are marked; they correspond to Events E8 and E12, respectively (Figure 12 and Table 2).